PERFORMANCE EVALUATION OF AN ACTIVE FILTER

NON-REGENERATIVE AC DRIVE

A Thesis

by

ALEX JOSEPH SKORCZ

Submitted to the Office of Graduate Studies of
Texas A&M University
in partial fulfillment of the requirements for the degree of

MASTER OF SCIENCE

December 2007

Major Subject: Electrical Engineering

PERFORMANCE EVALUATION OF AN ACTIVE FILTER

NON-REGENERATIVE AC DRIVE

A Thesis

by

ALEX JOSEPH SKORCZ

Submitted to the Office of Graduate Studies of
Texas A&M University
in partial fulfillment of the requirements for the degree of

MASTER OF SCIENCE

Approved by:

Chair of Committee,	Mehrdad Ehsani
Committee Members,	Hamid Toliyat
	Shankar Bhattacharyya
	Mark Holtzapple
Head of Department,	Costas Georghiades

December 2007

Major Subject: Electrical Engineering

ABSTRACT

Performance Evaluation of an Active Filter Non-Regenerative

AC Drive. (December 2007)

Alex Joseph Skorcz, B.S.E., Arkansas State University

Chair of Advisory Committee: Dr. Mehrdad Ehsani

The purpose of this work is to evaluate the performance of a specific ac drive topology that is of current interest in industry. With the increasing pressure for compliance with IEEE–519 and other international harmonic standards, many ac drive manufacturing companies are seeking innovative and cost effective solutions for controlling the amount of harmonics produced at the point of common coupling (PCC). The proposed topology is a potential alternative to the three-phase diode bridge which is the conventional rectifier topology for non-regenerative applications.

The work of this thesis explains the theory of operation, control algorithms, and potential improvement strategies for the proposed "half-controlled" boost rectifier topology. The entire ac drive system with load is then modeled and the results verified using the Simulink simulation package.

It is shown that the proposed topology has several distinct advantages over a traditional diode rectifier such as improved total harmonic distortion (THD) of the current waveforms, dc bus voltage regulation, and power factor control. In addition, these advantages are created at a price point which is significantly lower than that of a

conventional fully-controlled pulse-width modulated (PWM) rectifier. The main disadvantage is that the current waveforms in the utility contain even harmonics which may cause significant problems in the power system.

To my parents

ACKNOWLEDGEMENTS

I would first like to express my gratitude to Dr. M. Ehsani for his strong support, insight, and inspiration throughout the course of my graduate studies. I would also like to thank all of my committee members for the advice and assistance they offered me in order to complete this research. I am also very appreciative to the electrical engineering staff at Texas A&M for their dedication and support. I want to especially thank Ken Carr and David Benson for their devotion to this project. Without them, this project would have never left the ground. I am forever indebted to all of my current and former lab members from whom I've spent countless hours learning; especially Mr. H. Mena, Mr. B. Yancey, Mr. B. Nikbakhtan, Dr. P. Asadi, and Mr. D. Hoelscher. And last but not least, I want to thank my family for their unconditional support, guidance, and motivation throughout my studies.

TABLE OF CONTENTS

CHAPTER Page

Page

LIST OF FIGURES

FIGURE Page

FIGURE Page

LIST OF TABLES

CHAPTER I

INTRODUCTION: THE NEED FOR DRIVES

In this chapter we will explore the evolution of electric drives for motor control. A brief overview of electric drives will be presented which includes the need for drives and the benefits that they offer. All of the topics discussed are underlying factors that have motivated the existence and pursuit of this thesis work.

1.1 Overview

In general, the speed and torque of ac motors depend on the electrical quantities applied to the motor terminals. In the past, ac motors operated directly from the utility line at a fixed nominal voltage and a fixed frequency of 50 or 60 Hz. This fixed operating point limited the operation of the motors to essentially one corresponding speed. In order to change the speed, the motors need to be supplied with a variable voltage and variable frequency. This is achieved through an energy conversion process involving solid-state power devices and feedback controllers. The whole system together creates what is referred to as an adjustable speed drive (ASD) as shown in Fig. 1.1.

This thesis follows the style of *IEEE Transactions on Industry Applications.*

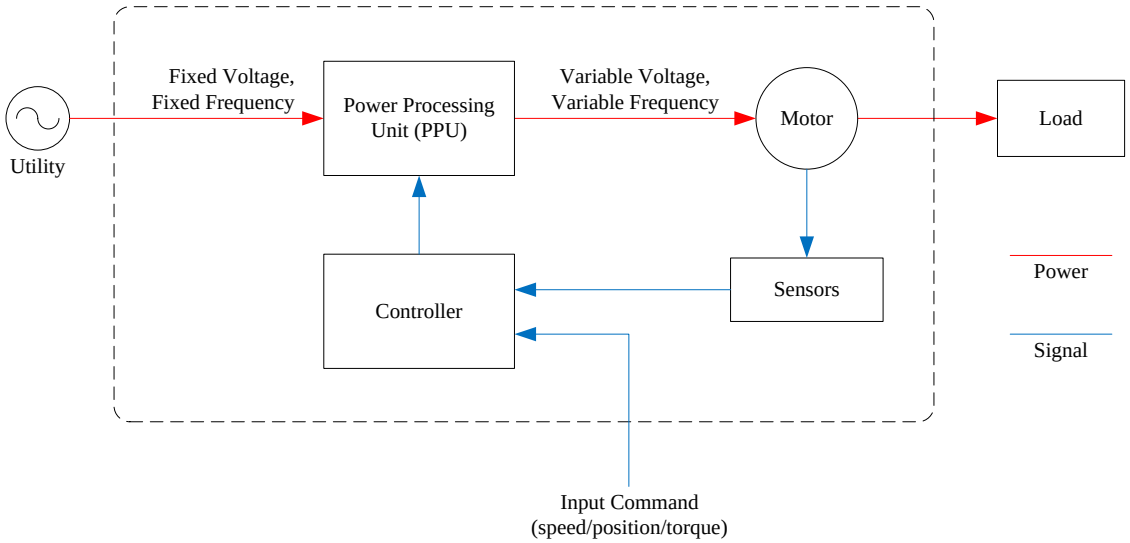

Fig. 1.1: Typical Adjustable Speed Drive System

1.2 The Increasing Use of Drives

The global market for ac drives was $10.7 billion in 2006 and is expected to increase to $16.1 billion by the year 2011 [11]. ASDs are very attractive from several perspectives including performance, energy usage, and long-term cost reduction. ASDs have the ability to supply the proper electrical quantities needed to the motor such that its operating point best suits the load. This is advantageous because it prevents the motor from doing more work than it needs to and because it also has the ability to compensate for rapid changes in the speed or torque of the load.

1.2.1 Solid State Electronics

In the past several decades, solid-state electronic devices have revolutionized the energy conversion process. The energy conversion process has become more efficient,

more sophisticated, and more economical than it once was. This is partially due to the continuous improvement of the voltage and current handling capabilities of power semiconductor devices. It is also a result of revolutionary advances in microelectronics which have enabled the use of high-speed digital controllers. The combination of these factors, as well as the decreasing cost, has lead to the acceptance and widespread use of electric drives for controlling the speed and/or torque of electric motors.

1.2.2 Energy Savings and Performance

Over one-half of all electric energy consumed in the United States is used by electric motors [4]. The total electric energy consumption in the United States for 2006 was 3,820 billion kilowatt-hours (kWh) [6]. The industrial sector, as a whole, spends more than $30 billion annually for electricity dedicated to motor-driven systems alone [5]. The United States Department of Energy (DOE) estimates that replacing line-fed electric motors used just in compressor and pump applications with ASD systems would improve the energy efficiency by 20%; enough energy to supply the entire state of New York for a year [2]. Fig. 1.2 illustrates the increasing demand for electric power in the U.S.

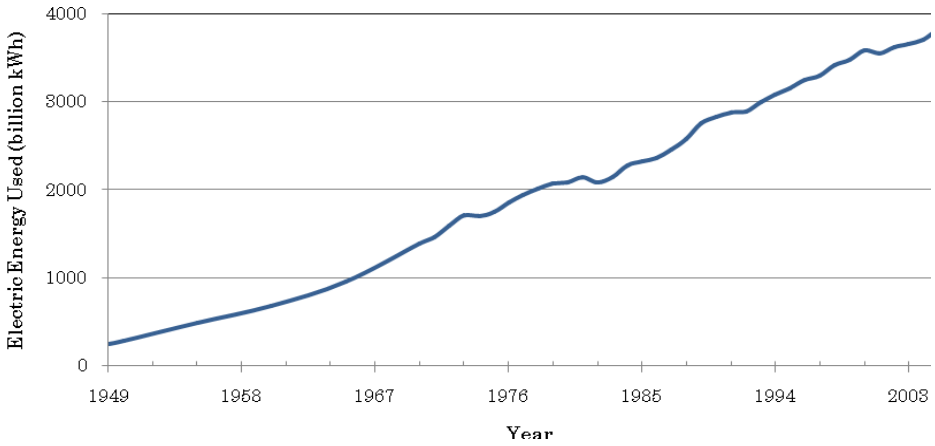

Fig. 1.2: The Increasing Electric Energy Demand in the U.S.

About one-half of the generated electric power in the U.S. comes from coal-powered generating plants. The overall efficiencies of coal-powered plants are in the range of 30 - 40% [7]. By taking into account the efficiency of coal power plants, it can be shown that the 20% energy savings at the utility grid side corresponds to roughly a 43% energy savings at the input of the power plant.

Many modern electric motor applications require very precise and high-performance position-controlled servo drives. Servo drives, a branch of ASDs, are needed in areas such as robotics. The response time and accuracy in which the motor follows the position commands are critical and would not be possible without the use of the electric drives. In addition to position-controlled servo motors, the performance of speed-controlled motors is also greatly improved using electric drives. In pump and compressor applications, the power required is usually proportional to the square or cube of speed. Therefore, a small reduction in speed may correspond to a significantly large reduction in the power demanded. This is illustrated in Fig. 1.3 below. Upon inspection,

it is shown that a 50% reduction in speed (flow) represents an 87.5% reduction in input power. Also, there are several applications which exhibit rapidly fluctuating loads. The uses of ASDs in these applications allow the motor to quickly respond to the load changes.

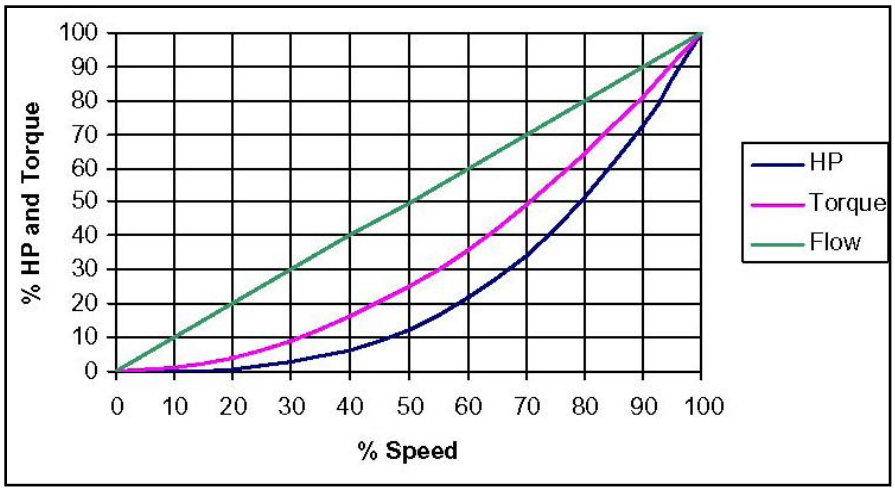

Fig. 1.3: Typical Pump Load Characteristics

1.3 The Disadvantages of Drives

As with most systems where advantages are present, there also exists corresponding disadvantages. From a customer's point of view, the biggest hurdle for implementing an electric drive system is the initial cost. From the supplier and utility point of view, one of the largest obstacles is controlling the amount of harmonics produced and injected into the utility power system. Both issues are very valid and are the topic of much of today's current research in this field.

1.3.1 Initial Cost

As shown in Fig. 1.4, the implementation of an ASD system usually constitutes a large upfront investment from the end user. As a general rule of thumb, basic ASDs cost about the same as the motors they drive, but they are highly dependent upon features and application requirements. Costs for basic drives start at around $520 per horsepower (HP) for a one HP drive and drop sharply to around $160 per HP for a 10 HP drive. Costs level off more slowly after that with 40 HP drives at about $100 per HP, and 500 HP drives down to about $70 per HP. Installation costs, electrical filters, and special features for constant torque, special controls, or diagnostics can easily more than double the costs [3].

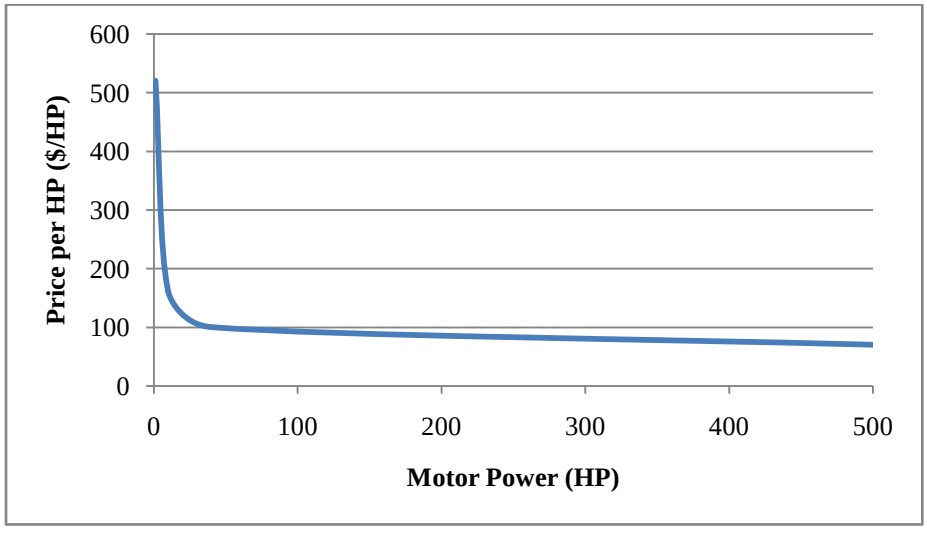

Fig. 1.4: Price Structure of Drives

Despite the large initial cost, ASD systems can present a very large long-term savings with a surprisingly short payback period. An example is presented in section 1.3.1.1 to express the savings encountered in a particular case study [12].

1.3.1.1 Case Study: Application of a 100 HP ASD Installation

Scenario:

- Three-phase electric motor, 100 HP, 92% efficient, driving a water pump [12]
- Power is proportional to cube of speed (flow): $P \propto \omega^3$
- Operates 20 hr/day:
    - 6 a.m. – 12 p.m.: 50% flow
    - 12 p.m. – 12 a.m.: 75% flow
    - 12 a.m. – 2 a.m.: 100% flow
    - 2 a.m. – 6 a.m.: 0% flow
- Electric Rate
    - \$0.05/kWh
    - \$5.0/kW, 8 a.m. – 10 p.m.

Present System:

- 20 hr/day at 100 HP (81 kW at input)
- Energy Use: $81\ kW \cdot 20\ hr/day \cdot 7\ day/wk \cdot 52\ wk/yr = 589{,}680\ kWh/yr$
- Electric Bill: \$28,477.20

With ASD

- 6 hr/day at 12.5 HP, 12 hr/day at 42.2 HP, 2 hr/day at 100 HP
- Energy Use: $230{,}412\ kWh/yr$
- Electric Bill: \$11,268.48

Summary of Results

- Cost Savings: \$17,178.72/yr

- Initial Cost: $15,000
- Payback Period: $\$15{,}000/\$17{,}178.72/yr = 0.87\ yrs \approx 10.5\ months$
- Drive is rated for 50,000 hrs life
    - Drive lasts about 7 yrs at 7280 hr/yr

1.3.2 Harmonics

The other major drawback to the use of drives that has drive designers and power system engineers concerned is the electrical pollution injected to the utility system from the drives. The power grid has to be shared by all and the use of drives by one customer may affect the quality of power delivered to all other customers at that particular point of common coupling (PCC) and beyond. This has sparked a great deal of research in academics, as well as industry, and has forced the creation of governing bodies to impose and standardize acceptable limits for harmonics generated from electric drives and other power converters.

1.4 Summary

The use of drives to control electric motors is rapidly increasing and the ASD market is ever-growing. ASDs are becoming more sophisticated, more efficient, more reliable, and more affordable. They offer numerous benefits over constant speed alternatives. In some cases, constant speed operation will not even complete the task being considered, thus requiring the use of an ASD. However, there are still issues concerning the use of ASDs, such as harmonics, that need to be addressed. The purpose of this thesis is to investigate a proposed ASD topology that could address these issues.

CHAPTER II

AC MOTOR DRIVES

In this chapter, conventional ac drives will be presented and discussed. Typical ac drive systems will first be discussed at a system level. Then, a more detailed investigation of each power conversion stage will be covered; focusing on rectification and inversion. Next, a brief overview of typical motor loads will be given, with an emphasis on permanent magnet synchronous machines (PMSM). Finally, power system harmonics will be introduced because they play a vital role in the design of most ac drive systems.

2.1 System Overview

As previously stated, the objective of an ac drive is to convert the fixed electrical quantities on the utility line into variable, yet controlled electrical quantities. In some cases, such as regenerative ac drives, it is also necessary to process the power in the reverse direction. That is, to take the variable electrical quantities and convert them into fixed frequency waveforms to be injected back into the power grid. In order to accomplish this conversion process, the electrical power must pass through three stages: rectification, storage, and inversion. Fig. 2.1 shows this process for a non-regenerative ac drive. For a regenerative drive, the arrows indicating the flow of power in Fig. 2.1 can be reversed.

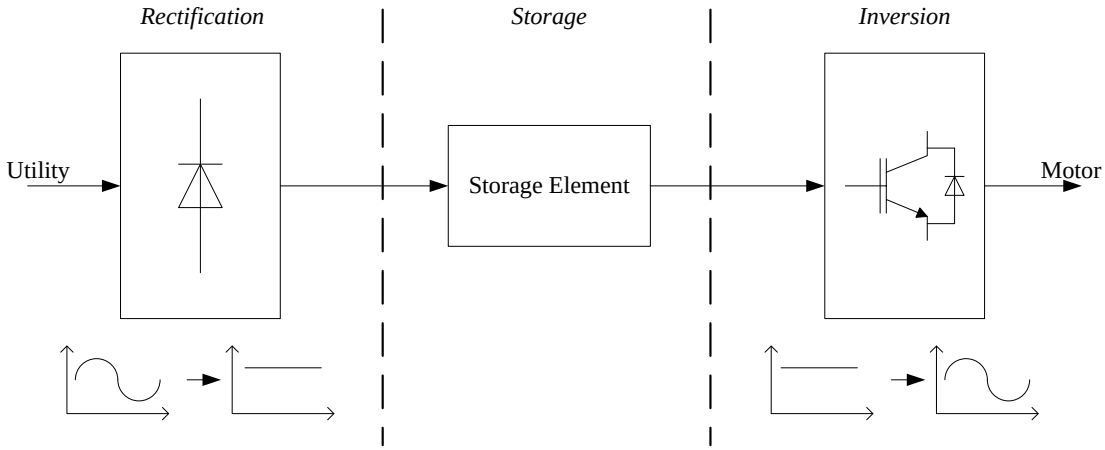

Fig. 2.1: Power Processing Stages

The rectifier stage uses power semiconductor devices to convert the fixed amplitude, fixed frequency ac from the utility to a nearly constant dc waveform. After rectification, the converted energy is then stored in an intermediate storage element which is usually a capacitor or inductor. The final stage again uses power semiconductor devices to convert the stored energy into a more suitable form to match the desired operating point of the electric motor. Each stage of the power conversion process will be covered in more detail in the following sections. There has been a great deal of research focused on each stage and this thesis focuses primarily on the rectification stage.

2.2 Rectifiers

Rectifiers constitute the first stage of power processing in an ac drive. Several topologies exist that each have their own advantages and disadvantages. The rectifier selection is an important part of the ac drive system because it is on the front side of the

drive and interfaces with the three-phase, sinusoidal utility. Therefore, input power quality versus cost becomes an important compromise in the design. All rectifiers can be classified as either regenerative or non-regenerative. This is illustrated in Fig. 2.2 below. The most commonly used rectifier topologies are the diode and voltage-source PWM rectifiers, which are discussed in the following sections.

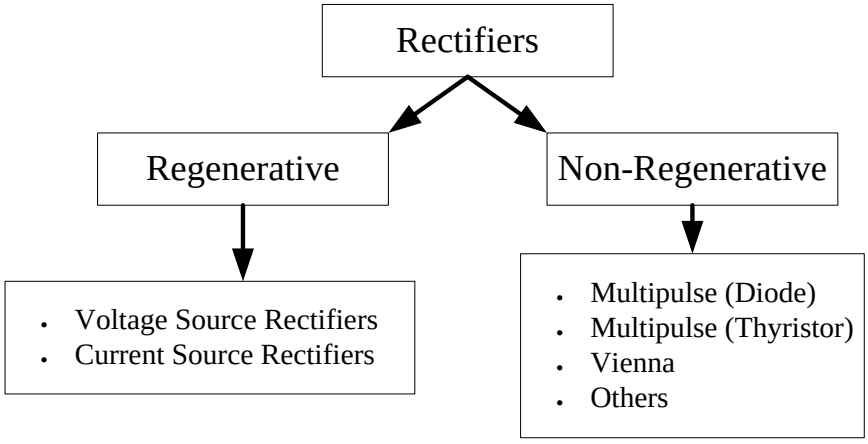

Fig. 2.2: Classification of Rectifiers

2.2.1 Three-Phase Diode Bridge Rectifiers

The typical ac drive without regenerative capabilities utilizes a three-phase diode rectifier, or “six-pulse” rectifier to convert ac voltages into a dc voltage (see Fig. 2.3). The use of these converters eliminates the control over the dc bus voltage and usually results in excessively high total harmonic distortion (THD) of the current waveforms (refer Fig. 2.4 and Fig. 2.5). The THD can be incrementally improved by increasing the amount of input inductance. However, this leads to a significant lagging power factor and a poor dynamic response. Despite these disadvantages, they are still widely used in

applications not requiring regenerative capabilities because of their simple structure, absence of control, and low cost.

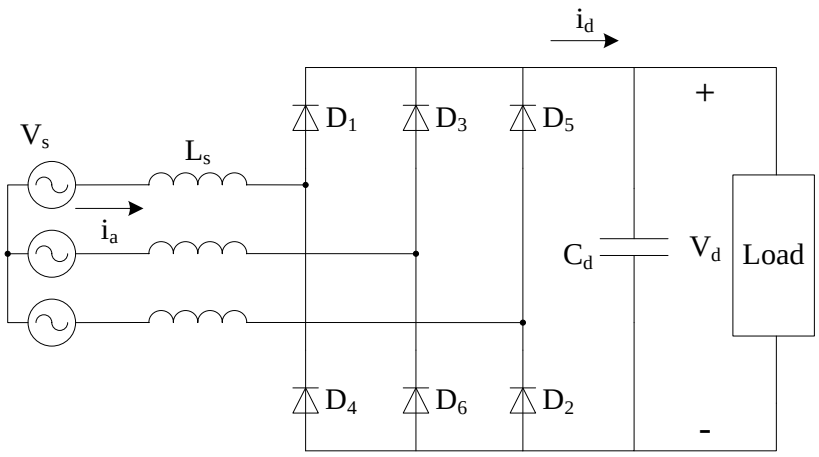

Fig. 2.3: Diode Bridge Rectifier Topology

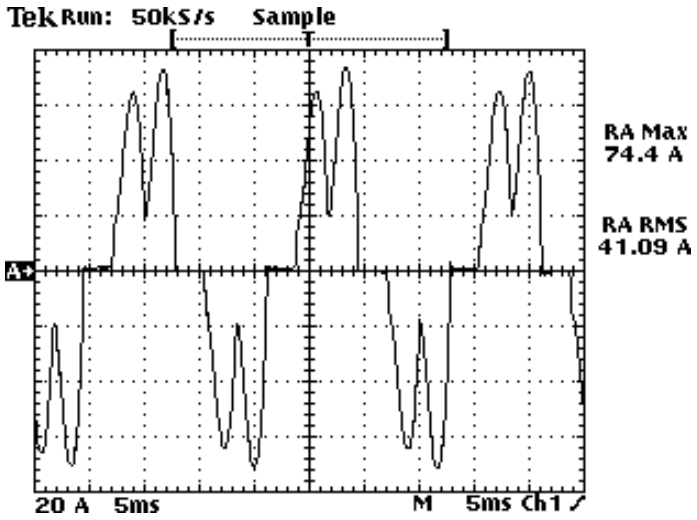

Fig. 2.4: Diode Bridge Line Currents with a 3% Input Inductance

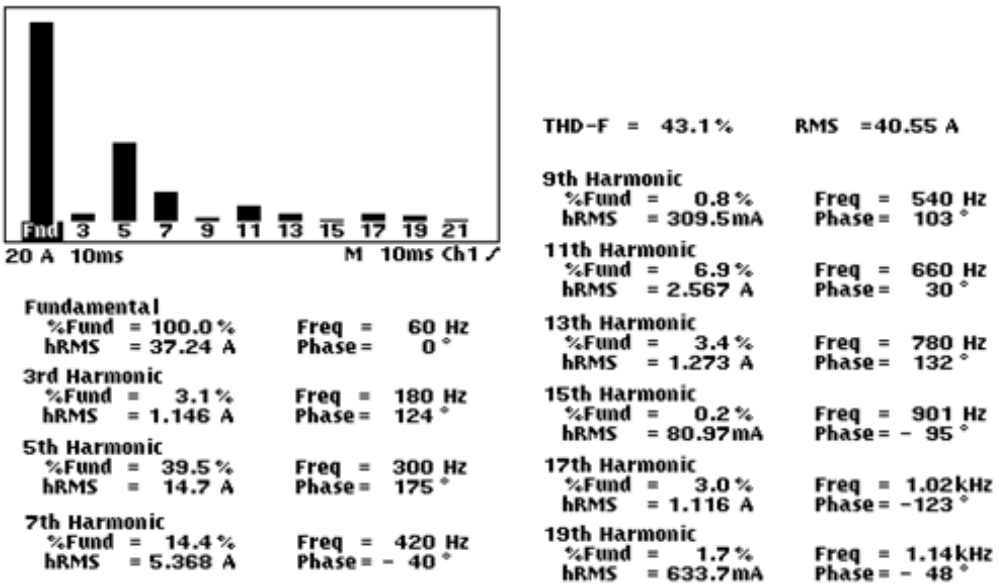

Fig. 2.5: Harmonic Components of Diode Bridge Input Currents with a 3% Input Inductance

2.2.2 Voltage-Source PWM Rectifiers

A typical ac drive with regenerative capabilities utilizes a voltage source PWM rectifier to convert ac utility voltages into a dc voltage (see Fig. 2.6).

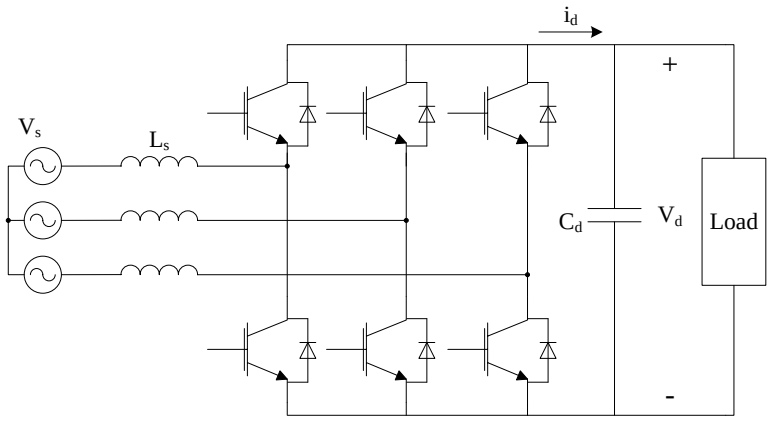

Fig. 2.6: Voltage-Source PWM Rectifier Topology

While these converters have a relatively high cost, they offer several advantages over an uncontrolled rectifier. This rectifier is able to regulate the dc bus voltage and maintain an optimal power factor for both power received and power delivered to the utility mains. In addition, the three-phase currents can be shaped to minimize the harmonic distortion which allows for compliance with IEEE – 519 Standards, as shown in Fig. 2.7 and Fig. 2.8.

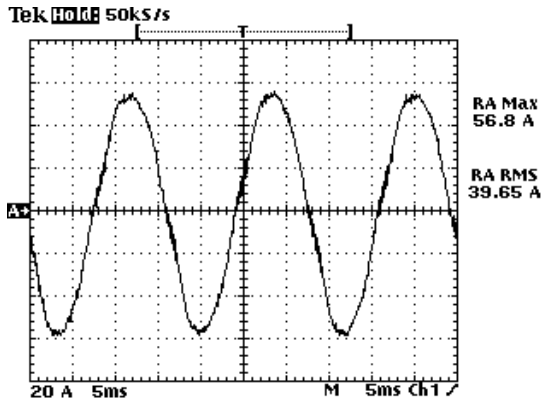

Fig. 2.7: PWM Rectifier Line Currents with 12% Input Inductance

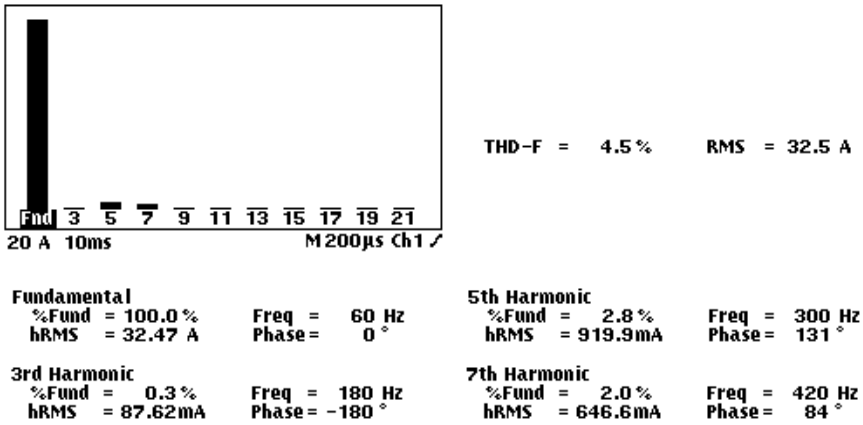

Fig. 2.8: Harmonics Components of PWM Rectifier Input Currents with 12% Input Inductance

2.2.3 Other Rectifiers

In addition to the most standard rectifier topologies, several others exist such as the Vienna rectifier shown in Fig. 2.9 and the Minnesota rectifier shown in Fig. 2.10. A modified Minnesota rectifier was developed by Ashida [22] and is shown in Fig. 2.11.

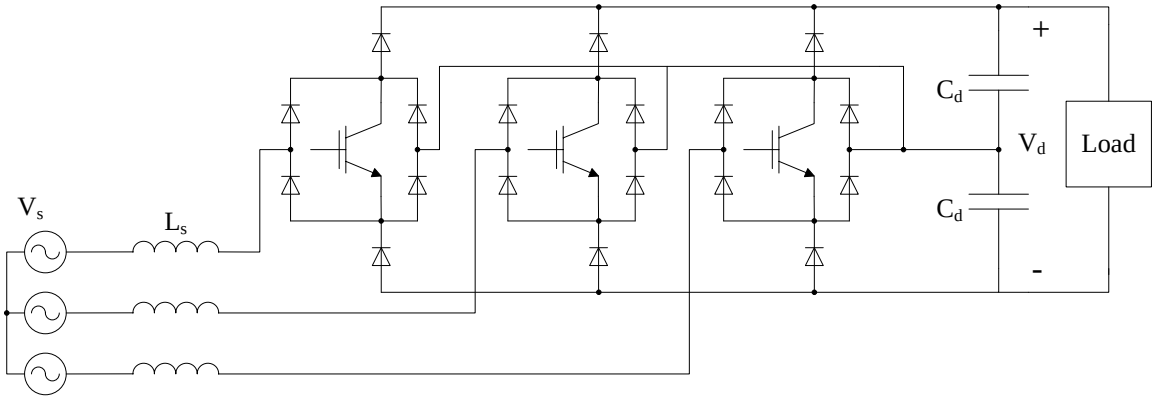

Fig. 2.9: Vienna Rectifier Topology

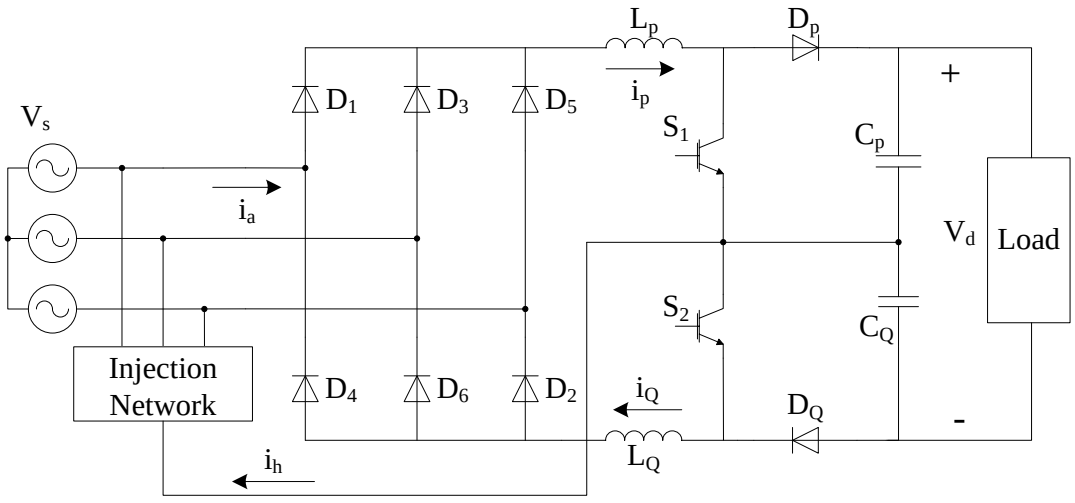

Fig. 2.10: Minnesota Rectifier

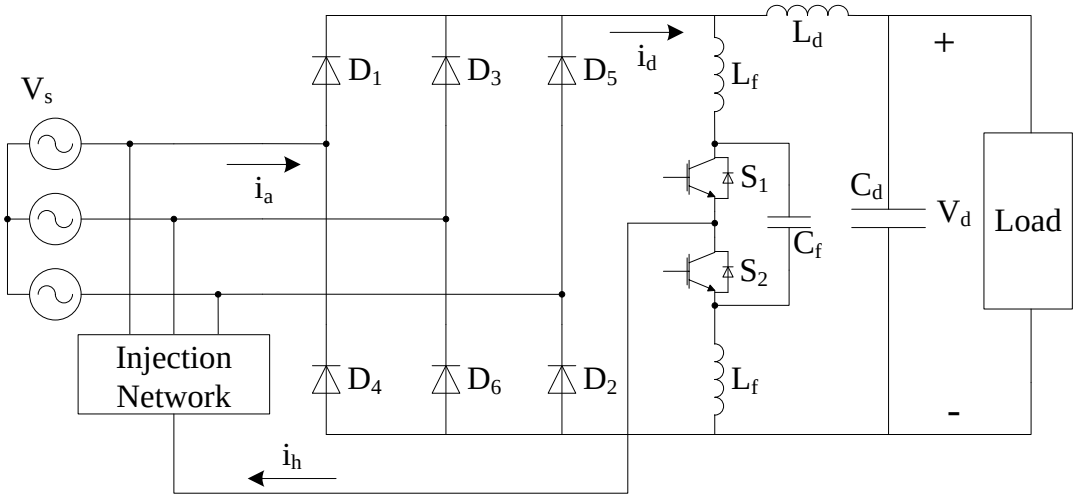

Fig. 2.11: Modified Minnesota Rectifier

All of these topologies offer significantly improved current waveforms compared to a diode rectifier, with fewer active components and a relatively low price point. They also feature power factor control. However, there are still some issues with their operation such as voltage balancing size which are topics of research.

2.3 Inverters

The inverter is responsible for converting the rectified dc voltage into variable frequency, variable amplitude ac waveforms that are best suited for the operating point of the electrical machine. There are two main types of inverters conventionally used in industry; voltage source inverters (VSI) and current source inverters (CSI). A brief description of each is given in the following sections

2.3.1 Voltage-Source Inverters

Voltage-source inverters, like the one shown in Fig. 2.12, are typically used for low and medium power applications to supply the motor with three-phase ac waveforms. The input to the inverter is a dc voltage, thus the name voltage-source inverter. There are two main types of VSIs; sine wave, or PWM, inverters and square wave inverters. The switches in a VSI operate at a much higher frequency than the fundamental frequency it produces. Therefore, the harmonics produced are usually very small. Since the input and output are isolated by the intermediate storage element, VSIs can supply a motor with a power factor that is mostly independent of the utility power factor.

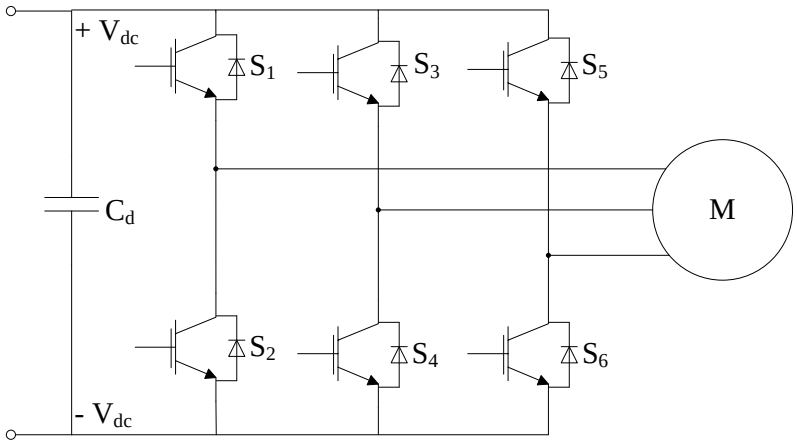

Fig. 2.12: PWM Voltage-Source Inverter

2.3.2 Current Source Inverters

Current source inverters are usually used in high power applications. CSIs require the use of a phase-controlled rectifier to produce a dc current (refer to Fig. 2.13).

The dc current is then used as the input to the inverter, and is then converted to a suitable three-phase ac current waveform.

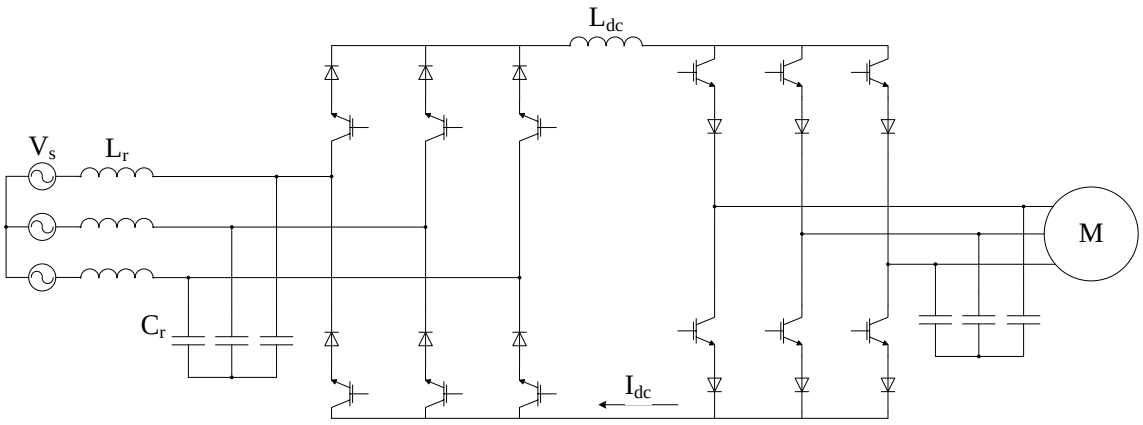

Fig. 2.13: Current Source Inverter

2.4 Motor Loads

There are several types of electric motors that require the use of ac drives. Some of the most well-known are induction, brushless dc (BLDC), wound-field synchronous, and permanent magnet synchronous machines (PMSM). Each machine has its own advantages and disadvantages. The induction motor is undoubtedly the most widely used electrical drive motor [20]. The induction motor with a squirrel cage rotor is one of the lowest cost machines to manufacture and it eliminates all brushes, resulting in an exceedingly simple and rugged construction. The permanent magnet machines (BLDC and PMSM) are more expensive machines because of the rare-earth magnets used, but offer higher torque-to-volume and torque-to-inertia ratios than induction machines. The latter makes them an excellent choice for servo applications. The BLDC is similar in

construction to the PMSM. The PMSM has a sinusoidal back emf and requires sinusoidal currents. The BLDC has a trapezoidal back emf and requires square-shaped currents which results in a higher torque ripple in the BLDC than the PMSM. For the purposes of this thesis, a PMSM motor is used as the load for the proposed ac drive system.

2.4.1 Permanent Magnet Synchronous Machine (PMSM)

The PMSM is quickly becoming the next-generation variable speed ac motor due to the availability of high-energy permanent magnet (PM) materials. It has widely found its application as a high performance machine drive because of its ripple-free torque characteristics and simple control strategies. Compared to induction machines, the PMSM has less rotor losses and hence it is potentially more efficient.

As mentioned in the previous section, the PMSM consists of permanent magnets on the rotor. They can be placed on the outside (exterior) or buried within (interior) the rotor. The stator has slots filled with sinusoidally distributed three-phase windings. For this reason, the stator should be supplied with three-phase sinusoidal currents. Fig. 2.14 shows a typical exterior PMSM configuration.

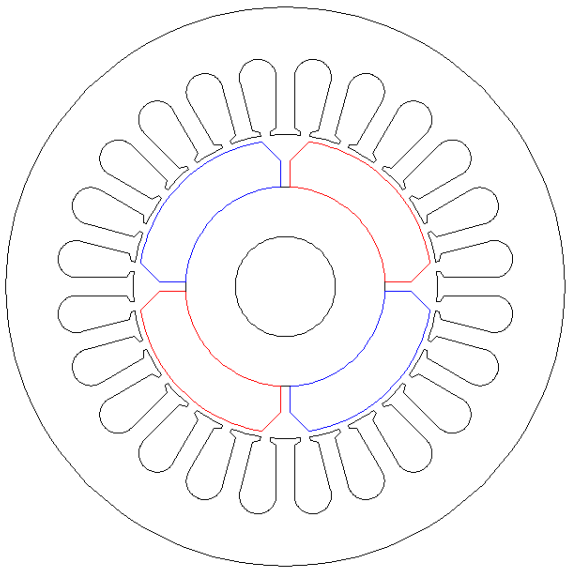

Fig. 2.14: Exterior PMSM Configuration

2.4.1.1 Mathematical Modeling

The mathematical model of a PMSM as viewed from a stationary reference frame can be expressed as (2.1). Note that the "s" subscripts indicate a stator quantity.

$$\begin{bmatrix} V_{as} \\ V_{bs} \\ V_{cs} \end{bmatrix} = R_s \cdot \begin{bmatrix} i_{as} \\ i_{bs} \\ i_{cs} \end{bmatrix} + \frac{d}{dt} \cdot \begin{bmatrix} \lambda_{as} \\ \lambda_{bs} \\ \lambda_{cs} \end{bmatrix} \tag{2.1}$$

Where V is the applied stator voltages, R_s is the stator resistance of each phase (ideally equal in each phase), i is the stator winding current in each phase, and λ is the flux linking each phase.

The flux linking each phase is a result of the current in the adjacent phases and also the flux produced by the permanent magnet λ'_m, as given in (2.2).

$$\begin{bmatrix}\lambda_{as}\\ \lambda_{bs}\\ \lambda_{cs}\end{bmatrix} = L_s \cdot \begin{bmatrix}i_{as}\\ i_{bs}\\ i_{cs}\end{bmatrix} + \lambda_m^{'} \cdot \begin{bmatrix}\sin(\vartheta_r)\\ \sin\left(\vartheta_r - \frac{2\pi}{3}\right)\\ \sin\left(\vartheta_r - \frac{4\pi}{3}\right)\end{bmatrix} \tag{2.2}$$

L_s in (2.2) is the self inductance in each phase winding and ϑ_r is the rotor position angle. The self inductance matrix L_s is given as (2.3) below.

$$L_s = \begin{bmatrix} L_{ls} + L_A - L_B\cos(2\theta_r) & -\frac{1}{2}L_A - L_B\cos\left(2\theta_r - \frac{2\pi}{3}\right) & -\frac{1}{2}L_A - L_B\cos\left(2\theta_r + \frac{2\pi}{3}\right)\\ -\frac{1}{2}L_A - L_B\cos\left(2\theta_r - \frac{2\pi}{3}\right) & L_{ls} + L_A - L_B\cos\left(2\theta_r - \frac{4\pi}{3}\right) & -\frac{1}{2}L_A - L_B\cos(2\theta_r + \pi)\\ -\frac{1}{2}L_A - L_B\cos\left(2\theta_r + \frac{2\pi}{3}\right) & -\frac{1}{2}L_A - L_B\cos(2\theta_r + \pi) & L_{ls} + L_A - L_B\cos\left(2\theta_r + \frac{4\pi}{3}\right)\end{bmatrix} \tag{2.3}$$

The torque equation of the machine can be expressed as (2.4).

$$\begin{aligned} T_e = \frac{P}{2}\Bigg\{\lambda_m^{'}\left[\left(i_{as} - \frac{1}{2}i_{bs} - \frac{1}{2}i_{cs}\right)cos\theta_r - \frac{\sqrt{3}}{2}(i_{bs} - i_{cs})sin\theta_r\right] \\ + \frac{L_{md} - L_{mq}}{3}\left[\left(i_{as}^2 - \frac{1}{2}i_{bs}^2 - \frac{1}{2}i_{cs}^2 - i_{as}i_{bs} - i_{as}i_{cs} + 2i_{bs}i_{cs}\right)sin2\theta_r\right. \\ \left. + \frac{\sqrt{3}}{2}(i_{bs}^2 i_{cs}^2 - 2i_{as}i_{bs} + 2i_{as}i_{cs})cos2\theta_r\right]\Bigg\} \end{aligned} \tag{2.4}$$

And finally, the torque and the rotor speed ω_{rm} can be related by (2.5); where J is the rotational inertia, B_m is the frictional coefficient, and T_L is the load torque.

$$J\frac{d}{dt}\omega_{rm} = \frac{P}{2}(T_e - T_L) - B_m\omega_{rm} \tag{2.5}$$

2.4.1.2 Rotating Reference Frame

It is obvious from the previous section that the PMSM is a complex and nonlinear machine. All of the equations given in section 2.4.1.1 were expressed in a stationary stator reference frame. The representation of the machine can greatly be simplified by transforming the three-phase system into a two-phase system. And it can be further simplified by attaching the frame of reference to the rotating rotor (see Fig. 2.15). These rotating axes are called the direct (d) and quadrature (q) axes.

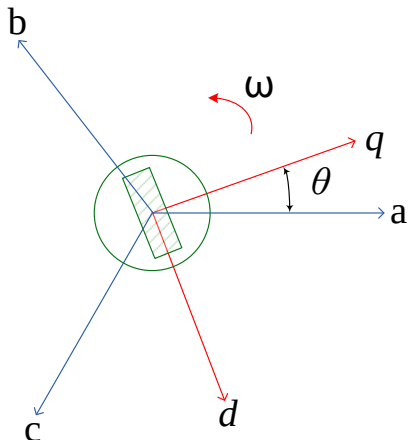

Fig. 2.15: Three-Phase to Two-Phase Transformation

The transformations used to obtain a rotating reference frame can easily be expressed as complex space vectors.

The transformation from a three-phase to an arbitrary two-phase system is given as (2.6) [23].

$$\underline{f}_{qds} = \frac{2}{3} e^{-j\theta} \left[f_{as} + \underline{a} f_{bs} + \underline{a}^2 f_{cs} \right] \tag{2.6}$$

Where,

$$\underline{a} = e^{j\frac{2\pi}{3}} \tag{2.7}$$

And f is the quantity being considered (voltage, current, flux, etc.). If the reference frame does not rotate, then $\theta = 0$ and (2.6) can be reduced to (2.8) and the reference is said to be fixed to the stator, which is represented by the "s" superscript.

$$\underline{f}^{s}_{qds} = \frac{2}{3} \left[f_{as} + \underline{a} f_{bs} + \underline{a}^2 f_{cs} \right] \tag{2.8}$$

To express the quantity in a rotational reference frame attached to the rotor, (2.9) must be used.

$$\underline{f}^{e}_{qds} = \underline{f}^{s}_{qds} e^{-j\theta_e} \tag{2.9}$$

Once the machine quantities are expressed in terms of rotating d and q components attached to the rotor, the mathematical model of the PMSM can be reduced to (2.10) – (2.12).

$$\frac{d}{dt}i_q = \frac{1}{L_q}v_q - \frac{r_s}{L_q}i_q - \frac{L_d}{L_q}P\omega_r i_d - \frac{\psi_m P\omega_r}{L_q} \tag{2.10}$$

$$\frac{d}{dt}i_d = \frac{1}{L_d}v_d - \frac{r_s}{L_d}i_d - \frac{L_q}{L_d}P\omega_r i_q \tag{2.11}$$

$$T_e = \frac{3P}{4}\cdot\left[\psi_m i_q - \left(L_q - L_d\right)\cdot i_d i_q\right] \tag{2.12}$$

2.4.1.3 Vector Control

Vector Control (VC) has several advantages over traditional speed control. VC works by directly controlling the machine flux and current vectors. Traditional ac drives control the output voltage and frequency, which indirectly controls the machine flux and torque. The torque response of the electrical machine can be ten times faster with VC than with speed control. VC is ideal for servo and actuator applications requiring precise position and torque control.

2.5 Power System Harmonics

Due to the numerous reasons stated in Chapter I, the use of electric drives and other power conversion stages are proliferating. This increasing use of nonlinear switching semiconductor devices has created many problems regarding the power quality of the utility system. In general, power electronic converters demand non-sinusoidal waveforms from the utility line, resulting in the generation power system harmonics. Therefore, it is important to understand and consider harmonics in the design

of ac drive systems. This section will attempt to present the fundamentals necessary to analyze and understand harmonic related issues.

2.5.1 Harmonics Defined

Harmonics are components of a distorted periodic voltage or current waveform whose frequencies are integer multiples of the fundamental frequency [8]. The term "harmonics" was originated in the field of acoustics, where it was related to the vibration of a string in an air column at a frequency that is a multiple of the base frequency [9]. The presence of harmonics in a power system indicate that either the voltage or the current waveform, or both, are distorted resulting in the term "harmonic distortion." Fig. 2.16 illustrates several typical harmonic waveforms.

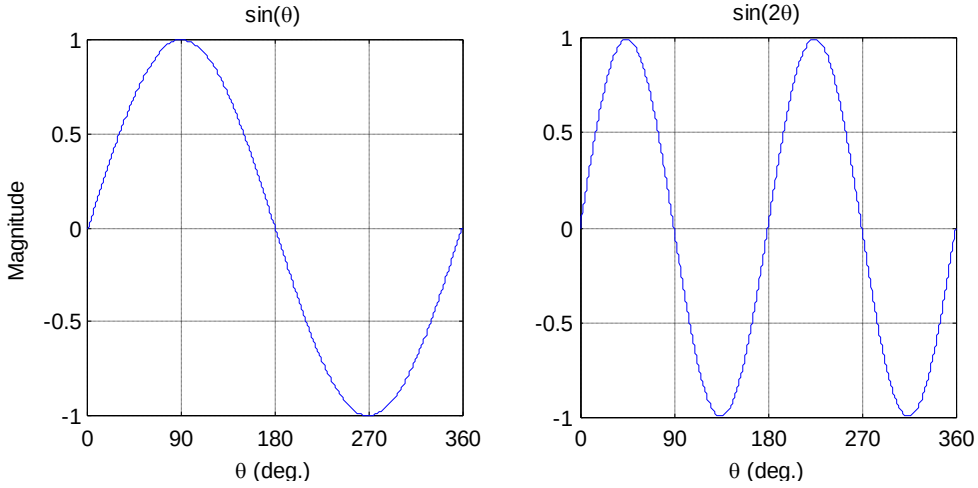

Fig. 2.16: Typical Harmonic Waveforms

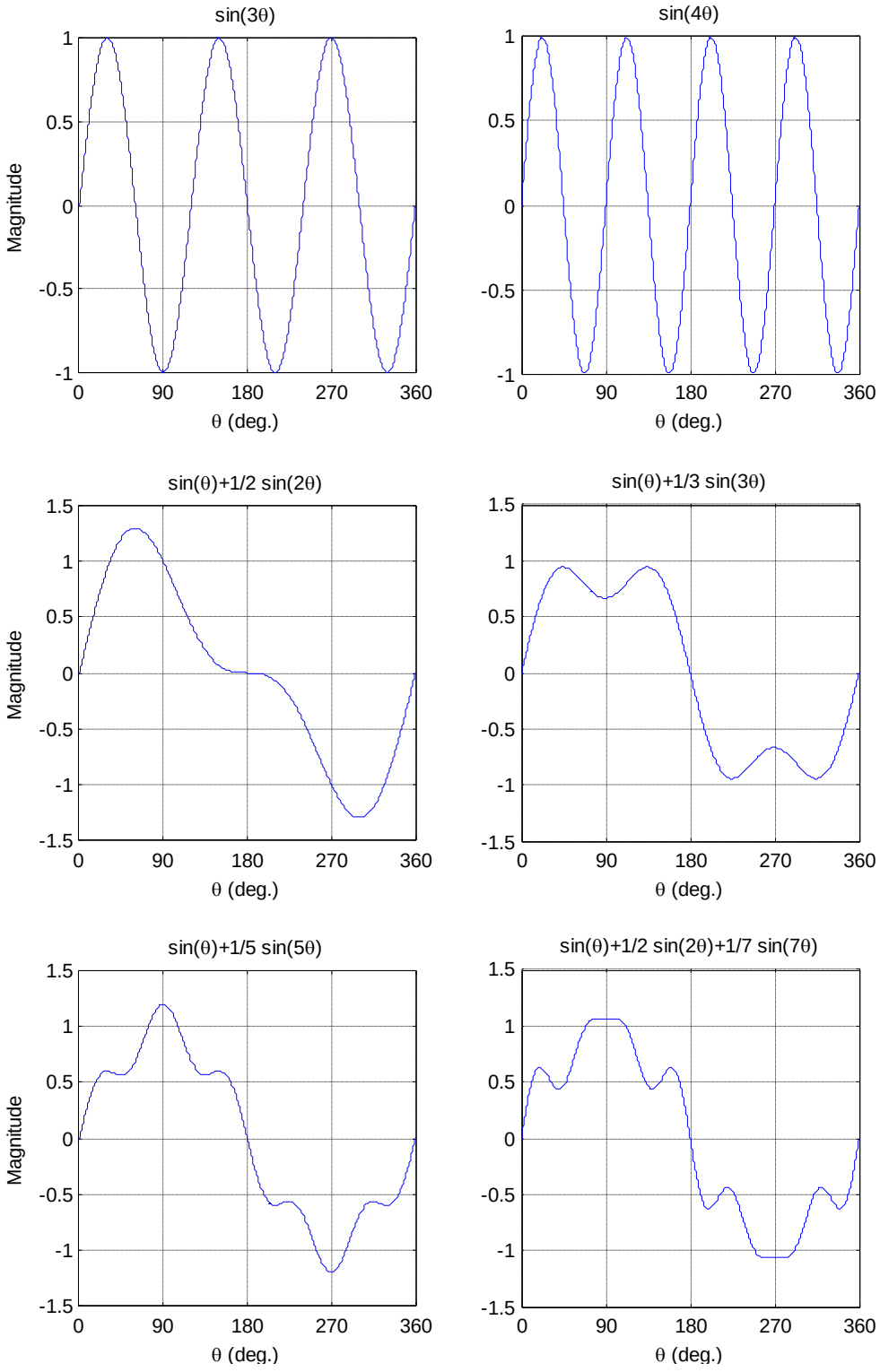

Figure 2.16 continued

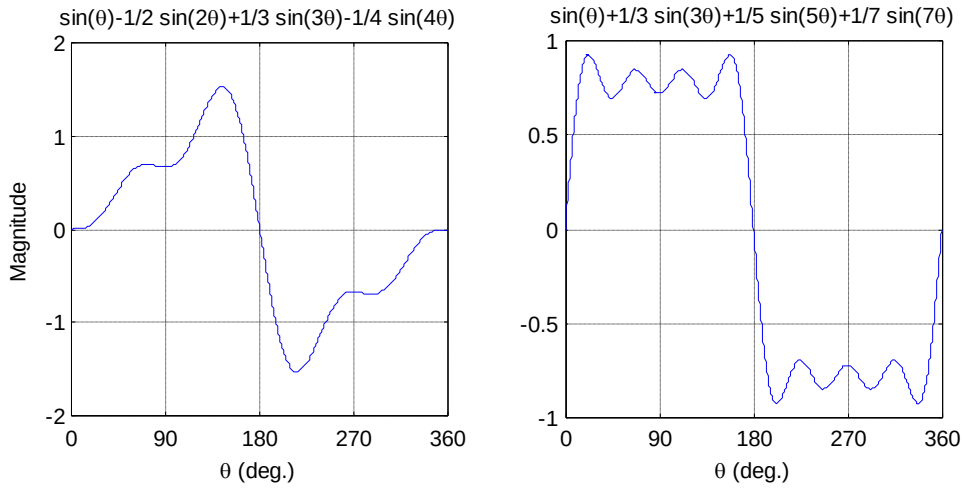

Figure 2.16 continued

2.5.2 Sources of Harmonics

Harmonic distortion is no longer a phenomenon confined to industrial equipment and processes, where the first power quality concerns developed. Uninterruptable power supplies (UPS's), personal computers, consumer electronics, entertaining devices, and electric drives are all contributors to the harmonic distortion problem [9]. Harmonic distortion results in increased equipment heating and losses that shorten the lifetime of sensitive loads. In the power system, harmonics cause increased losses and interference with protection, control, and communications circuits [8]. They also increase the level of total power demanded.

2.5.3 Odd and Even Harmonics

Odd harmonics are the characteristic harmonic components in modern power systems due to the three-phase symmetry of the present infrastructure. The signature of

odd harmonics, even though there is distortion, represents a symmetrical waveform. Symmetry in a power system waveform is very important. Even harmonics, on the other hand, suggest that the waveform is not symmetric. Asymmetric waveforms in the power system can have a more harmful impact than symmetric waveforms. Asymmetry implies that the positive and negative peaks are unequal. Fig. 2.17 compares a waveform that contains an even harmonic with a waveform that contains an odd harmonic. It is important to notice that the waveform containing the even harmonic has unequal peaks, and the waveform containing the odd harmonic remains symmetric despite its distortion.

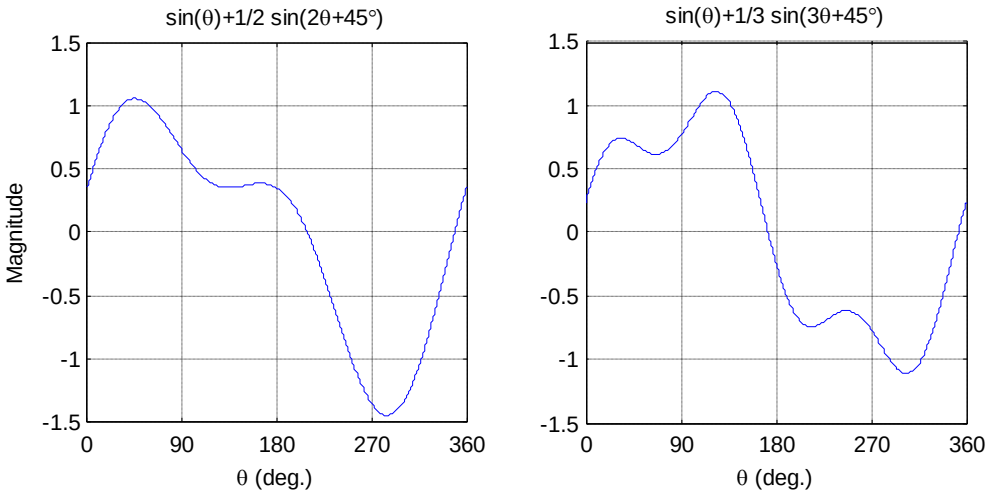

Fig. 2.17: Comparison of Waveforms Containing Even and Odd Harmonics

The unequal peaks translate to an asymmetrical transversal of the B-H curve for transformers; thus resulting in a dc offset (see Fig. 2.18). For this reason, governing bodies such as IEEE and International Electrotechnical Commission (IEC) impose more stringent standards on the acceptable levels of even harmonics.

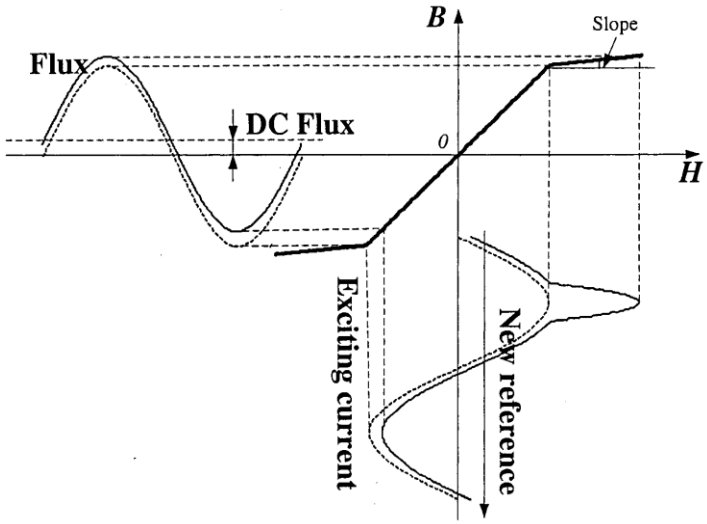

Fig. 2.18: Generation of DC Components in a Transformer

2.5.4 Three-Phase Harmonics

Three-phase systems, due to their configurations, have distinct harmonic signatures. A four-wire, Y-connected system is shown in Fig. 2.19. In a four-wire system, harmonic currents can lead to large currents in the neutral conductors which may easily exceed the rms rating of the mains. Power factor correction capacitors may also experience increased rms currents which can lead to their failure. For a four-wire system, it can be shown that the neutral currents contain only triplen harmonics [15]. All other frequencies cancel out as shown in (2.13).

$$i_n(t) = 3I_0 + \sum_{h=3,6,9,\ldots}^{\infty} 3I_h \cos(h\omega t - \theta_h) \tag{2.13}$$

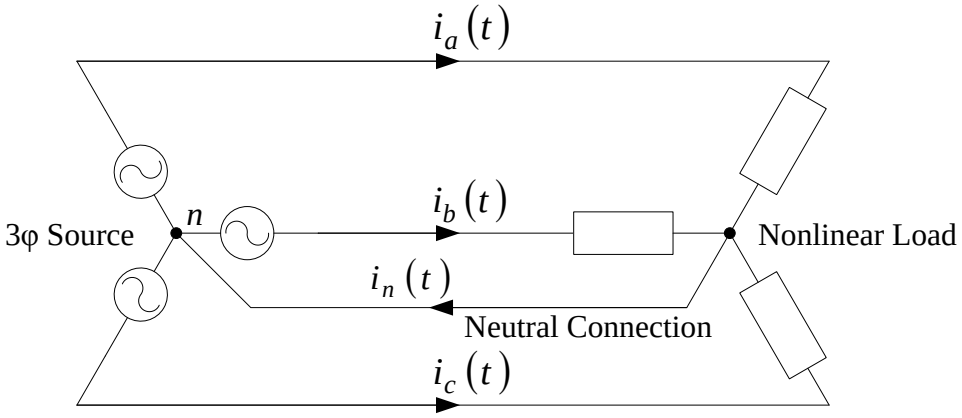

Fig. 2.19: Four-Wire Y-Connected System

In a three-wire system, $i_n(t) = 0$ since there is no neutral connection (see Fig. 2.20). Without the neutral connection, there is no path for the triplen harmonics to flow. Therefore, an ideal three-wire system will always lack triplen harmonics and a dc offset.

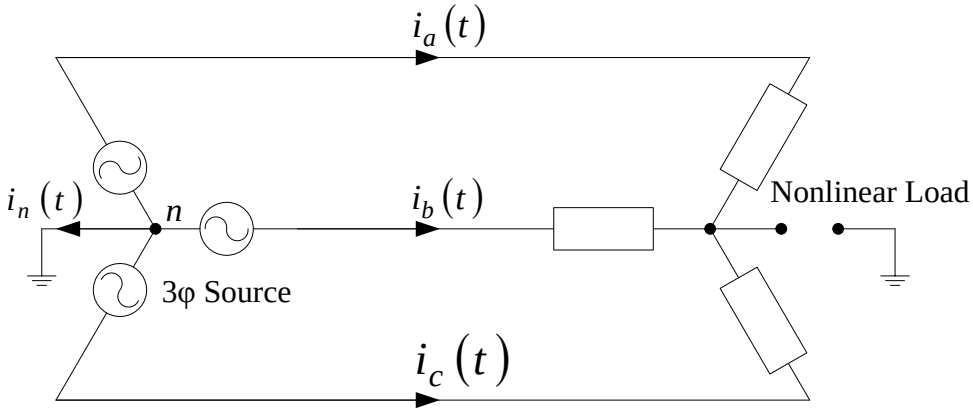

Fig 2.20: Three-Wire Y-Connected System

Similar to the three-wire system, a delta-connected load (see Fig. 2.21) also has no direct neutral connection; thus the ac lines contain no dc or triplen harmonic components. However, it is possible that these components may be circulating within the delta.

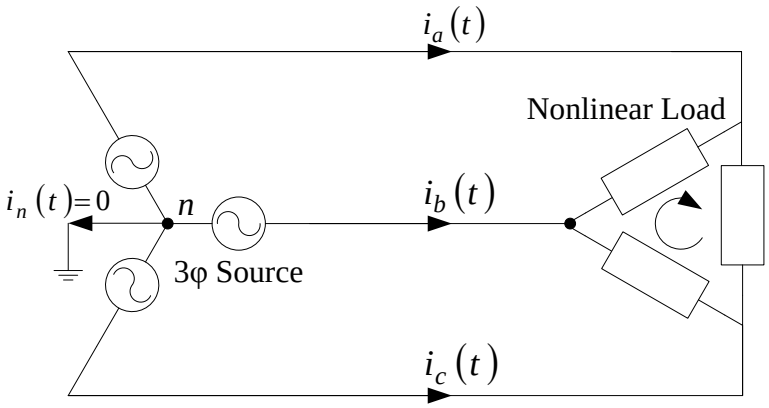

Fig. 2.21: Three-Wire Delta-Connected System

2.5.5 The Fourier Series

The Fourier series has become the method of choice for effectively analyzing and representing harmonic waveforms. By definition, a function $f(t)$ is periodic when $f(t) = f(t+T)$, where T is the period. The Fourier series states that, as long as the Dirichlet conditions are met, a periodic function $f(t)$ can be represented by a trigonometric series of elements consisting of a dc component and other elements having frequencies comprising the fundamental component and an infinite number of its integer multiples. The Dirichlet conditions are as follows [9]:

(1) If a discontinuous function $f(t)$ has a finite number of discontinuities over the period T.

(2) If $f(t)$ has a finite mean value over the period T.

(3) If $f(t)$ has a finite number of positive and negative maximum values.

Assuming these conditions are met, any periodic $f(t)$ can be expressed as the following trigonometric series:

$$f(t) = A_0 + \sum_{h=1}^{\infty} [A_h \cos(h\omega_0 t) + B_h \sin(h\omega_0 t)] \tag{2.14}$$

Where $\omega_0 = 2\pi/T$. The coefficients A_0, A_h, and B_h are referred to as the Fourier coefficients and are defined in (2.15), (2.16), and (2.17), respectively:

$$A_0 = \frac{1}{T}\int_0^T f(t)\, dt \tag{2.15}$$

$$A_h = \frac{2}{T}\int_0^T f(t) \cos(h\omega_0 t)\, dt \tag{2.16}$$

$$B_h = \frac{2}{T}\int_0^T f(t) \sin(h\omega_0 t)\, dt \tag{2.17}$$

It is also useful to represent (2.14) above as:

$$f(t) = A_0 + \sum_{h=1}^{\infty} C_h \sin(h\omega_0 t + \phi_h) \tag{2.18}$$

$$C_h = \sqrt{{A_h}^2 + {B_h}^2} \tag{2.19}$$

$$\phi_h = tan^{-1}\left(\frac{A_h}{B_h}\right) \tag{2.20}$$

2.5.6 Power Quality Indices

Several terms have been developed and are recognized as useful in describing harmonic distortion in any power system. Since the distorted voltage or current contains individual harmonics that contribute to the overall non-sinusoidal waveform, the rms value must be computed using (2.21).

$$F_{rms} = \sqrt{\sum_{h=1}^{\infty} F_{h,rms}^2} \tag{2.21}$$

Where F can be either the voltage or current being considered. Fig. 2.22 presents a distorted line current waveform and identifies key parameters used in analysis.

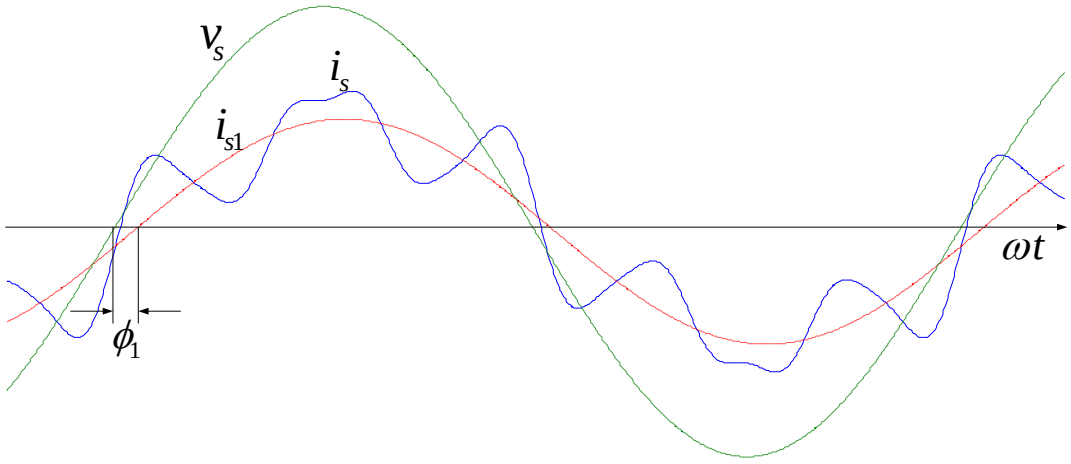

Fig. 2.22: Line Current Distortion

Total harmonic distortion (THD) is likely the most commonly used measure of power system quality. THD is a representation of the amount of non-fundamental frequency components present in a waveform. It is a key index for defining the effect of harmonics on the power system voltage or current and is given in (2.22) below.

$$THD_F = \sqrt{\sum_{h\neq 1}^{\infty} \left(\frac{F_h}{F_1}\right)^2} \tag{2.22}$$

It is important to note that the THD represents the total distortion of a waveform and gives no insight as to which particular harmonic multiples may be present. For this reason, Liu and Heydt [13] suggest the indices total even harmonic distortion (TEHD) and total odd harmonic distortion (TOHD), given by (2.23) and (2.24) respectively.

$$TEHD_F = \frac{\sqrt{\sum_{h\geq 1}^{\infty}[F_{2h}^2]}}{F_1} \tag{2.23}$$

$$TOHD_F = \frac{\sqrt{\sum_{h>1}^{\infty}[F_{2h-1}^2]}}{F_1} \tag{2.24}$$

The THD can then be expressed in terms of TEHD and TOHD as shown in (2.25).

$$THD_F = \sqrt{(TEHD_F)^2 + (TOHD_F)^2} \tag{2.25}$$

The power factor (PF) of a distorted waveform and the displacement power factor (DPF) are given as (2.26) and (2.27), respectively.

$$PF = \frac{F_1}{F_{rms}} \cdot \cos\phi_1 \tag{2.26}$$

$$DPF = cos\phi_1 \tag{2.27}$$

2.5.7 Harmonic Standards

IEEE has become the prominent governing organization for all things electrical in the U.S. Likewise, the IEC has become the governing organization for most European countries. In order to quantify and set limits for harmonic pollution, both organizations have created standard documents for their respective power systems. Both standards are mature documents that have pushed, and continue to push, companies towards compliance not only for the overall health of the power system, but also the health of

individual customer's loads. A brief overview of each is can be found in Table 2.1 and Table 2.2

2.5.7.1 IEEE-519-1992

Table 2.1: IEEE Current Harmonic Limits (120V-69kV) [13]

Maximum Harmonic Current Distortion in Percent of I_L						
Individual Harmonic Order (Odd Harmonics)						
I_{sc}/I_L	< 11	11 ≤ h < 17	17 ≤ h < 23	23 ≤ h < 35	35 ≤ h	TDD
< 20*	4	2	1.5	0.6	0.3	5
20 < 50	7	3.5	2.5	1	0.5	8
50 < 100	10	4.5	4	1.5	0.7	12
100 < 1000	12	5.5	5	2	1	15
> 1000	15	7	6	2.5	1.4	20
Even Harmonics are limited to 25% of the odd harmonic limits. TDD refers to Total Demand Distortion and is based on the average maximum demand current at the fundamental frequency, taken at the PCC.						
* All power generation equipment is limited to these values of current distortion regardless of I_{sc}/I_L.						
I_{sc} = Maximum short circuit current at the PCC I_L = Maximum demand load current (fundamental) at the PCC h = Harmonic order						

2.5.7.2 IEC 61000-3-6

Table 2.2: IEC Current Harmonic Limits [10]

Harmonics [h]	Class A [A]	Class B [B]	Class C [% of fund.]	Class D [mA/W]
Odd Harmonics				
3	2.3	3.45	30 x λ	3.4
5	1.14	1.71	10	1.9
7	0.77	1.155	7	1
9	0.4	0.6	5	0.5
11	0.33	0.495	3	0.35
13	0.21	0.315	3	0.3
15≤h≤39	0.15 x 15/h	0.225 x 15/h	3	3.85/h
Even Harmonics				
2	1.08	1.62	2	-
4	0.43	0.645	-	-
6	0.3	0.45	-	-
8≤h≤40	0.23 x 8/h	0.345 x 8/h	-	-

2.5.8 Harmonic Mitigation

The mitigation of harmonics is a rapidly growing research field. It is in fact the reason for this thesis. In general, proposed techniques can be broadly classified at passive solutions or active solutions. However, rather than employ additional circuitry to compensate, it is better to prevent harmonics in the first place by design. A more detailed investigation will be provided in the next three sections.

2.5.8.1 Passive Solutions

Passive filters have been used for harmonics mitigation purposes for a long time [8]. They consist of capacitors, inductors, and damping resistors tuned to specific harmonic frequencies [16]. Passive filters provide a low impedance path for a particular harmonic to which the filter is tuned. Several types of passive filters exist, as shown in Fig. 2.23.

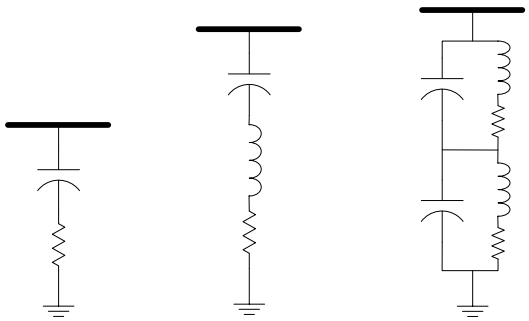

Fig. 2.23: Passive Harmonic Filters: (i) Damped (ii) Series-tuned (iii) Double band-pass

Passive filters have several disadvantages. They are dependent on the source impedance and they are inadequate for filtering non-characteristic frequencies such as even harmonics or those caused by non-ideal system and/or load unbalance. Moreover, they are usually very bulky and require a large amount of additional space.

2.5.8.2 Active Solutions

Active harmonic filters (AHF) have become a viable alternative for controlling harmonic levels in industrial and commercial facilities [17]. The AHF concept uses power electronics to produce harmonic components which cancel the harmonic components from the nonlinear loads. Two broad categories of AHFs exist: series-connected and shunt (parallel) connected. The shunt AHF (Fig. 2.24) is the most widely used because its configuration requires it to only process the harmonic (reactive) power, which is usually only around 25% of the rated load power. Typical shunt AHF waveforms are shown in Fig. 2.25.

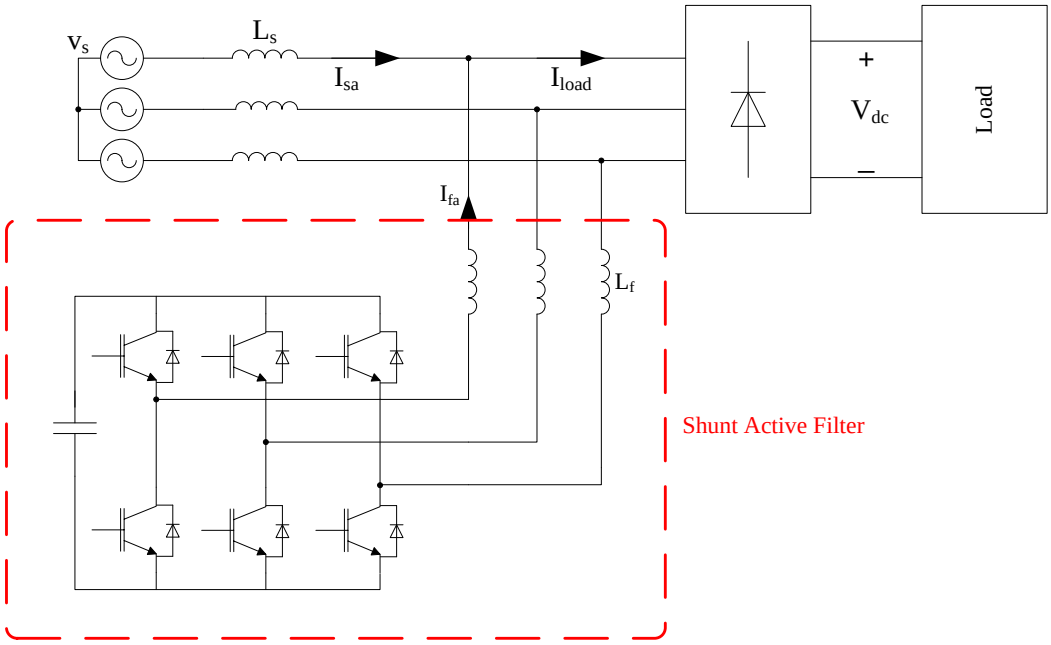

Fig. 2.24: Shunt-Connected Active Harmonic Filter Configuration

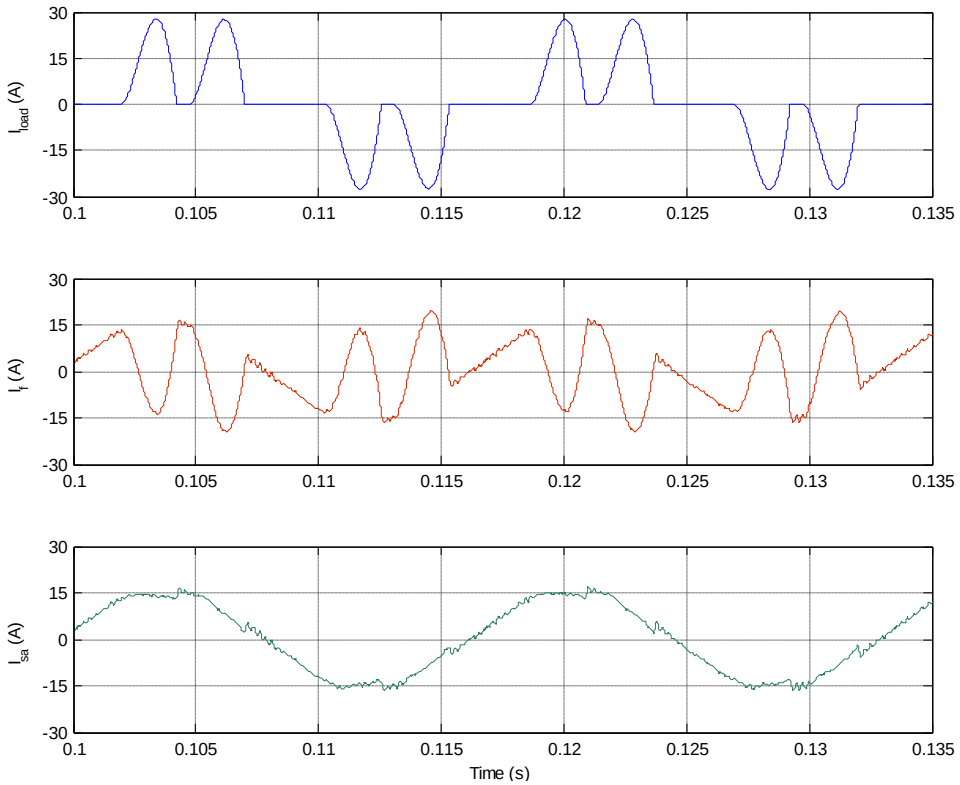

Fig. 2.25: Shunt Active Harmonic Filter Waveforms

2.5.8.3 Harmonic Prevention

Harmonic filters, passive or active, can be beneficial to ensure clean power within a system. However, changing and improving the characteristics of nonlinear devices by design can reduce the amount of produced harmonic in some cases, thus eliminating the need for extra filters. Improvements can be made in two of the most harmonic-producing loads: rectifier/inverter systems and dc power supplies.

CHAPTER III

PROPOSED AC DRIVE TOPOLOGY

In this chapter, the proposed ac drive will be presented. The principles of operation and control strategy will be discussed. The implementation of the system into the Simulink simulation package will be described and verified. The final section of this chapter will briefly explain creating and modeling the PMSM load operating under vector control (VC) for use in the ac drive system.

3.1 Overview

As expressed in Chapter II, the voltage-source PWM rectifier is the high performance and high cost solution while the diode bridge is the low performance and low cost solution for rectifier topologies in ac drives. The proposed topology presented in this chapter is a middle-of-the-road alternative that could provide higher performance than the typical three-phase diode bridge at a lower cost than the PWM rectifier. The proposed topology is given in Fig. 3.1.

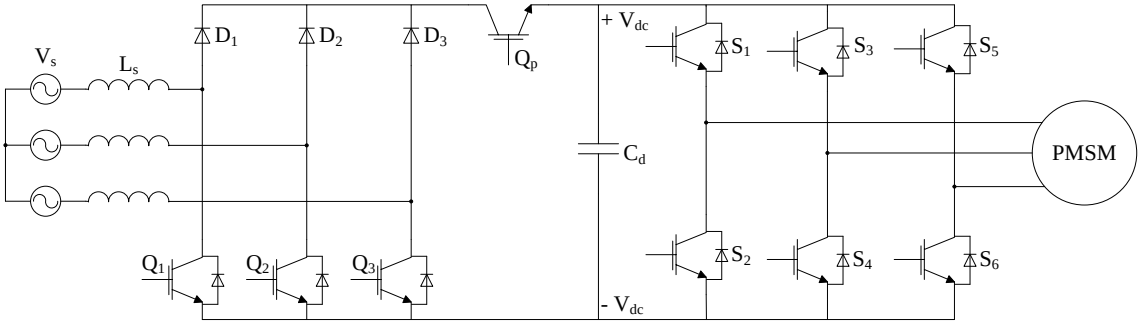

Fig. 3.1: Proposed AC Drive Topology

Upon inspection, the most obvious distinction between the proposed topology and a PWM rectifier is the reduction of three switches. In addition to the reduced switch cost, there also exists an associated reduced power supply cost. PWM rectifiers conventionally have four isolated power supplies to drive the gates: one for each of the upper switches and one for all of the three lower switches. Because the lower three switches have a common emitter configuration, this topology only requires one isolated power supply for operation.

Upon further inspection, it can be realized that the proposed topology is basically a three-phase boost converter. For that reason, the proposed configuration is capable of controlling the dc bus to a boosted level. However, when the dc bus is below the peak of the ac mains, the rectifier acts as a standard three-phase diode bridge. That is, the dc bus voltage cannot be controlled from 0V to approximately $\sqrt{2} \cdot V_{LL}$ unless switch Q_p is employed, which may lead to discontinuous conduction mode in the dc link.

Furthermore, the proposed topology is capable of controlling the power factor from leading to lagging as determined by the control system. The main disadvantage, however, is that there are two regions per waveform in the negative half-cycle where the control is briefly lost. This situation results in waveform asymmetry which leads to the generation of even-order harmonic multiples. All of these characteristics will be discussed in more detail in the following sections.

3.2 Theory of Operation and Control

The overall circuit operation is very similar to a boost converter. Consider a sinusoidal current in phase a. During the positive half-cycle of the waveform, switch Q_1 can be closed (see Fig. 3.2) to short-circuit the voltage V_{ab} across the input inductance. This causes the current in phase a to rise and energy to be stored in the input reactor. Then, when Q_1 is opened, the input current must instantaneously be continuous in Ls. Therefore, D_1 becomes forward-biased and the energy stored in the input inductance is transferred to the dc bus capacitance.

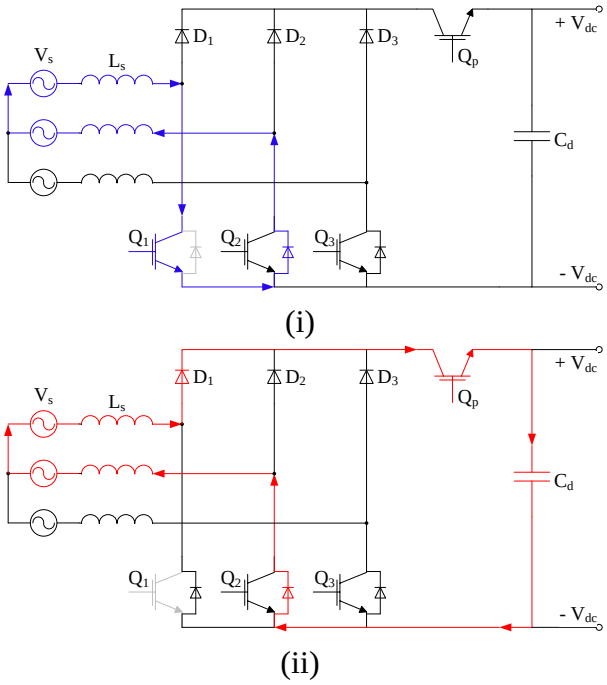

Fig. 3.2: Circuit Operation: (i) Q_1 closed (ii) Q_1 opened

This strategy works well for positive half-cycle current shaping. However, there are certain regions of the waveform, namely the negative half-cycle, where control cannot be maintained. If we consider Fig. 3.1, it can be seen that the only conduction path in any phase that allows negative half-cycle current is through the corresponding anti-parallel diode in the lower-leg of that particular phase. The diode is passive and its conduction is controlled mostly by the phase voltages, not the control system. Because of this, the current waveform cannot be regulated around a reference in certain negative half-cycle regions. The reasons why can be explained by the inspecting the symmetry of a three-phase system, as shown in Fig. 3.3.

The symmetry of three-phase systems guarantees one of the following two conditions is met at any given time:

(1) two waveforms are positive and one is negative (sectors I, III, and V)
(2) two waveforms are negative and one is positive (sectors II, IV, and VI)

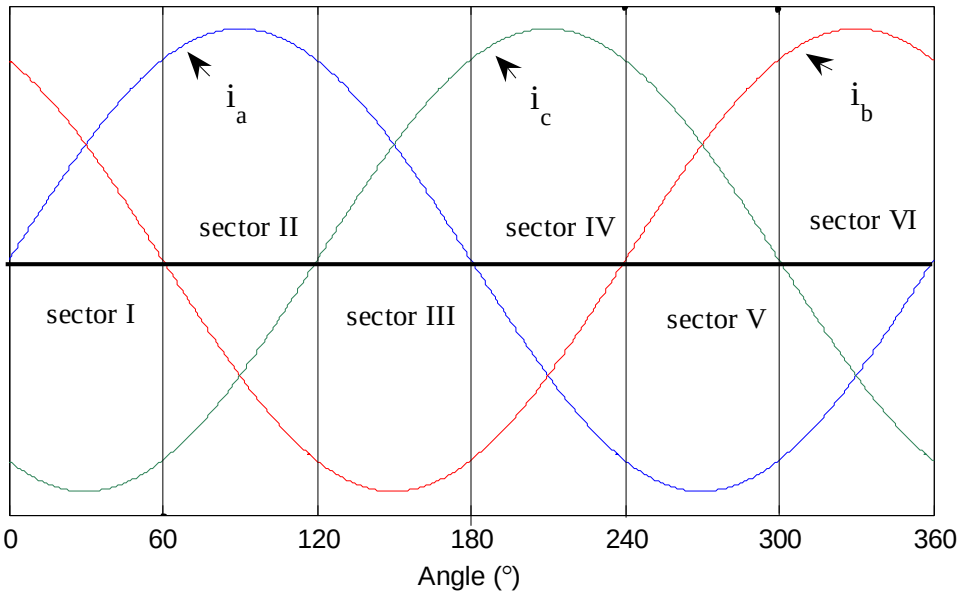

Fig. 3.3: Operating Sectors of Proposed Topology

It has already been shown that there are no active elements to control the current in the negative half-cycle. However, due to the fact the system has a wye-connected three-phase source, Kirchoff's current law (KCL) requires the sum of i_a, i_b, and i_c to equal zero. Therefore, in sectors I, III, and V, even though the negative current cannot be directly controlled, it is indirectly controlled by the two positive controlled currents and the KCL constraint. In sectors II, IV, and VI, the only controlled current is the one in its positive half-cycle. Controlling one of three currents is not enough to force the other phases to be regulated and thus the two negative currents are uncontrolled.

3.3 Modeling the System

To fully understand the behavior of the proposed topology, the system and its control was modeled and simulated. The simulations verify the initial assumptions and provide insight into the way different parameters affect the overall operation of the drive. The following system parameters were assumed:

- 240 V, three-phase source, wye-connected
- 5 HP drive/motor
- 12 kHz rectifier switching frequency
- Inverter-driven PMSM load
    - 15.2 full-load amps (FLA)
- 375 V desired dc bus

3.3.1 Simulink Overview

The Simulink package is a MATLAB subset. It is well-known and highly regarded as one of the best power electronics simulation programs in industry. For most power electronics circuitry, the SimPowerSystems toolbox can be used. This add-on toolbox contains accurate models for insulated-gate bipolar transistors (IBGTs) switches, three-phase sources, converters, electrical machines, and many other commonly used system components. Simulink also offers a wide range of logic and control blocks that can easily be implemented in reality using a DSP or microcontroller.

3.3.2 Rectifier

To begin initial investigations into the rectifier operation, we can consider the system to be in steady state. That is, the dc bus capacitance is assumed to be precharged to the desired voltage. Also, the load is assumed to be a static load absorbing FLA. This can be best modeled with a constant current source as shown in Fig. 3.4. After initial operation and control is verified, a more realistic and dynamic load is developed to complete the modeling of the entire system and will be discussed in Section 3.3.4.

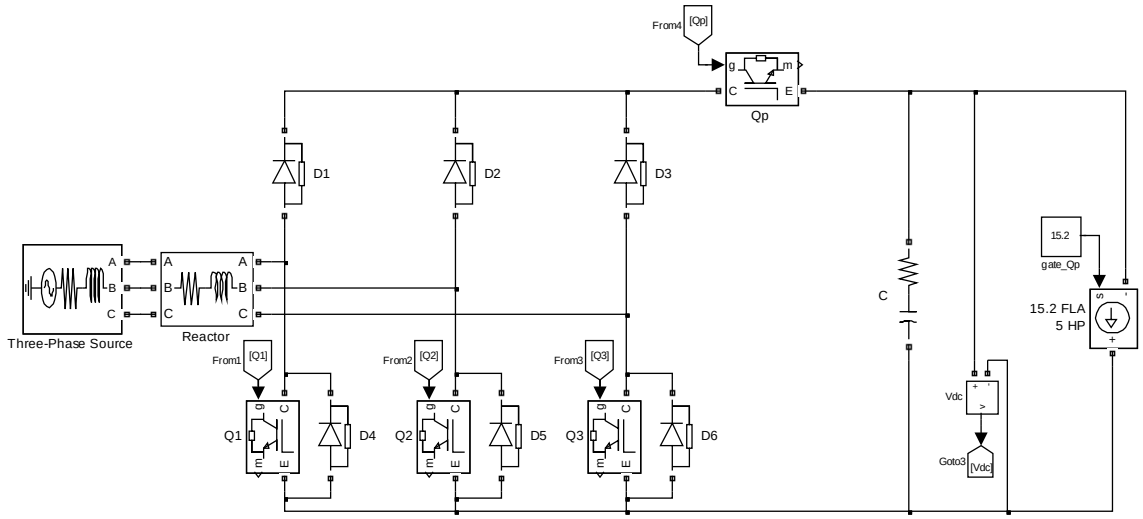

Fig. 3.4: Steady-State Model of Proposed Drive

The dc bus capacitor is modeled as an RC element to represent the equivalent series resistance (ESR) of the capacitor. The input inductance is modeled as an RL element to account for the series resistance as well. Furthermore, the source is also modeled with an impedance to account for the utility line inductance and short-circuit capability.

3.3.3 Control System

There are several control objectives for the proposed drive. First and most importantly, we want to control the shape of the line currents entering the rectifier. Simultaneously, we want to control the dc voltage level and also the power factor of the received current. And finally, we want to control the dc link current during startup so that large inrush currents are prevented. In order to obtain all of these control objectives, it was necessary to separate the control into several different parts.

The most inner control loop is the current control loop because it has the fastest dynamics. Since the behavior of the rectifier is similar to the well-known boost converter, it is reasonable to assume that the current can be controlled by PWM techniques. By changing the duty cycle, *D*, the average current can be increased or decreased (see Fig. 3.5). There are several current controlling techniques that are well-known. The most simple and robust method for a two-state converter is to use a hysteresis current controller. However, hysteresis control is a variable switching frequency type of control. The switching frequency depends largely on load parameters and varies with the input ac voltage, and protection of the converter is difficult because of the somewhat random switching [19]. The use of a linear PI control is satisfactory if the low harmonics of current command are well below $^1/_9$ of the carrier frequency. In this case, the desired carrier is fixed at 12 kHz. Therefore, the 60 Hz fundamental frequency of the utility to be rectified is well below the limit of 1.33 kHz and will be used to control the proposed drive.

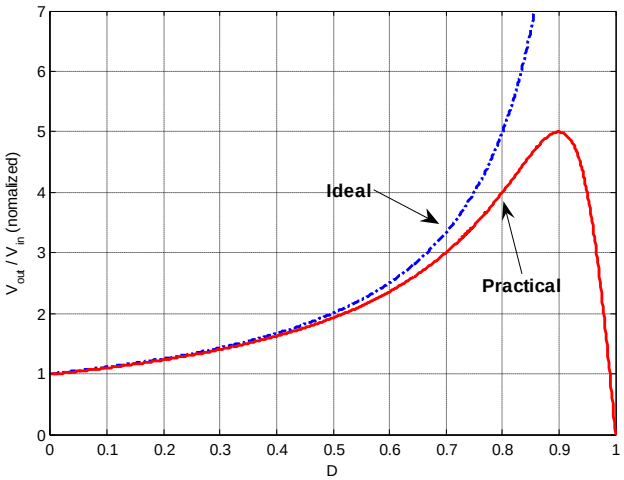

Fig. 3.5: Boost Converter Characteristics

The next control objective is the dc bus voltage. Relative to the current, the dc bus voltage is slow because of the energy storage in the capacitor. Therefore, the voltage control loop is the outer control loop. The voltage control is a two part control loop. First, it is important to realize that the voltage control loop determines the current reference for the inner loop. For this reason, the outer loop needs to determine the amplitude, shape, and phase shift of desired current. The amplitude of the command current regulates the amount of charge injected to the dc bus capacitance by the current, and thus regulates the level of dc bus voltage, as given in (3.1).

$$V_{dc} = \frac{1}{C} \cdot \int_0^t i \, dt \tag{3.1}$$

The shape of the command current should be sinusoidal to eliminate harmonics and the phase angle of the command current should be small to ensure a superior power factor. By multiplying the commanded amplitude of the current with a unit sine wave having a particular phase angle, the current command in each phase can be generated. An overview of the control system just discussed is given in Fig. 3.6.

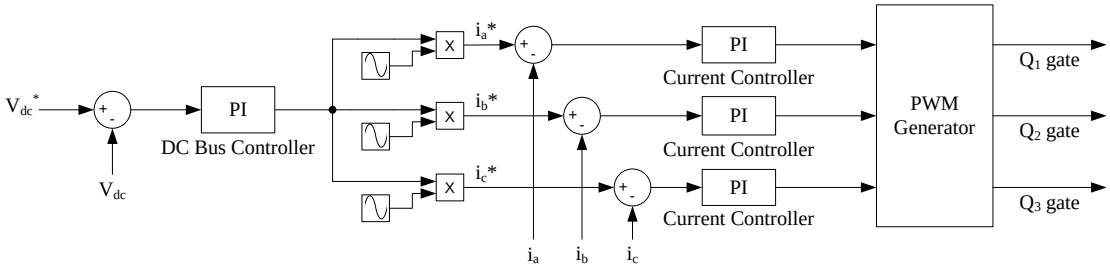

Fig. 3.6: Control Overview

In addition to the steady-state control just presented, a separate control loop needs to be implemented to control the precharge switch Q_p. The switch is responsible for limiting the inrush current at low bus voltages and should only be controlled when the dc bus voltage is less than $\sqrt{2} \cdot V_{LL}$. The upper limit of inrush current was selected to be 20 A and simple hysteresis (bang-bang) control with is used to regulate it, as shown in Fig. 3.7.

Since Q_p is located in series with the dc link, the problem is that there is no alternative path of conduction for the current. Therefore, opening and closing Q_p creates discontinuous current conduction. Without a careful snubber circuit design, the reverse voltages created by L_s become excessively large. Therefore a simple RC snubber design was implemented to allow a parallel path of current around the switch and prevent the current discontinuities.

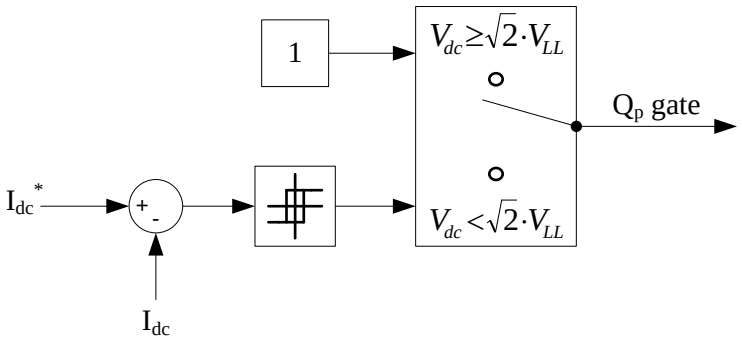

Fig. 3.7: Q_p Control Blocks

3.3.4 Inverter-Driven PMSM

While the focus of this thesis is on the rectification stage of the ac drive, it is also important to analyze the behavior of the entire system with a dynamic load. Industry has

shown particular interest in using the proposed topology in servo drive applications. The servo motor of choice is the PMSM. Therefore, a standard PWM voltage source inverter will be used to control a PMSM with the characteristics given in Table 3.1. The model implemented in Simulink is illustrated in Fig. 3.8.

Table 3.1: PMSM Specifications

Parameter	Value	Units
V_{dc}	300	V
T_r	24	N·m
P	4	pairs
ω_r	2300	r.p.m.
R_s	0.0918	Ω
L_d	0.975	mH
L_q	0.975	mH
ψ_m	0.1688	Wb
J	3.945×10^{-3}	$kg \cdot m^2$
B	0.4924	N·m·s

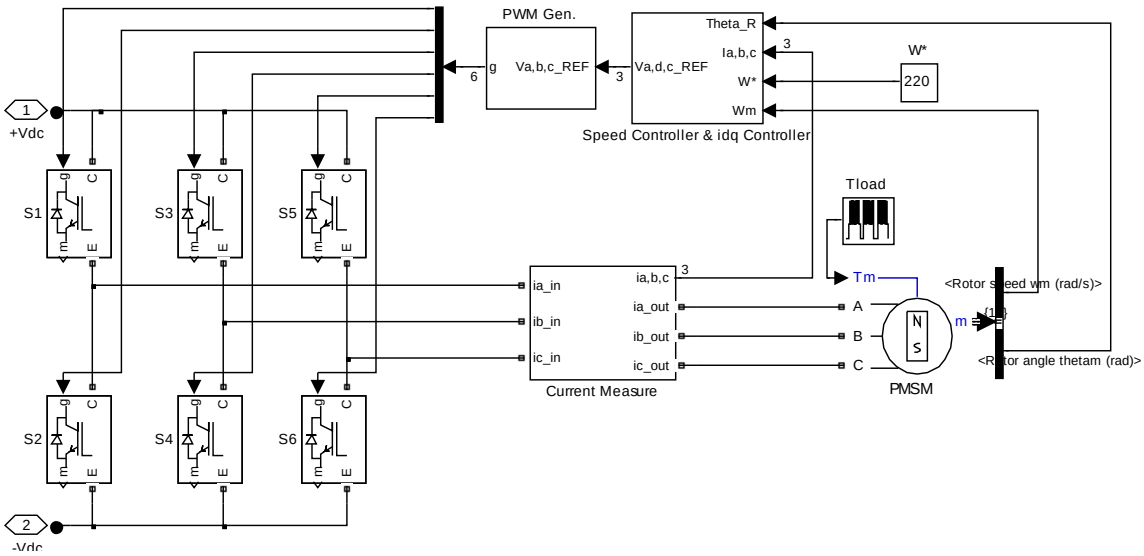

Fig. 3.8: Inverter-Fed PMSM Model in Simulink

3.3.4.1 Vector Control

Vector control is implemented to control the PMSM. As discussed in section 2.4.1.3, PMSMs are prime candidates for VC. The control implemented is illustrated in Fig. 3.9. The direct axis current is commanded to be zero which provides a torque angle of 90°. This results in the torque being directly proportional to the quadrature axis current.

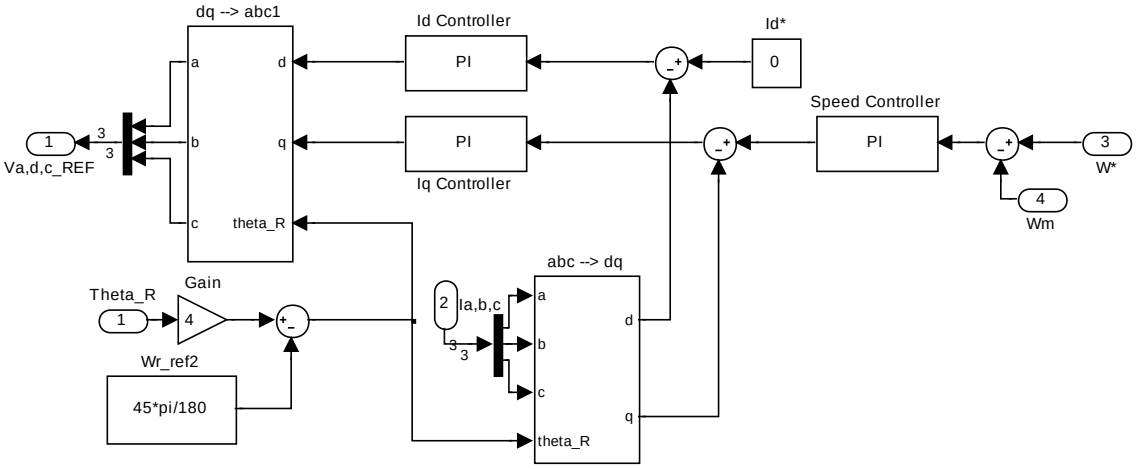

Fig. 3.9: Implementation of VC for PMSM

3.3.4.2 Model Results

The results of the inverter-fed PMSM load are shown in Fig. 3.10 and Fig 3.11. The speed ramps up to a value of 220 rad/s and is then held constant. The control is responsible for holding the constant speed while the load torque fluctuates every 25 ms. The torque and speed responses are excellent, and the PMSM operation and control are verified for use as components in the proposed ac drive system.

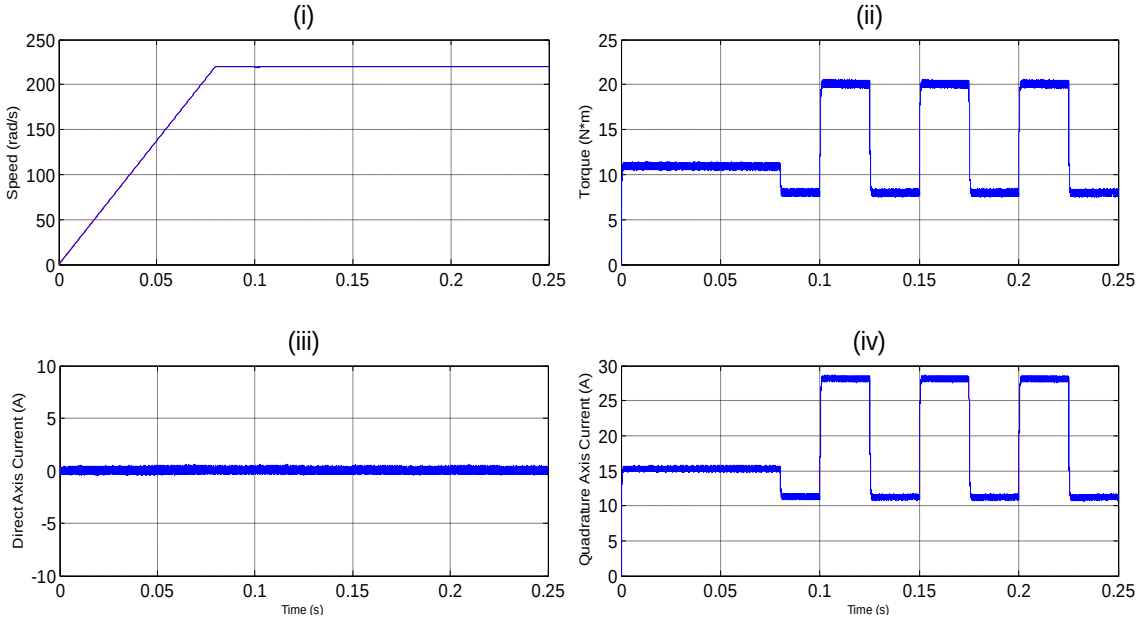

Fig. 3.10: PMSM Verification: (i) Speed (ii) Torque (iii) Direct Axis Current (iv) Quadrature Axis Current

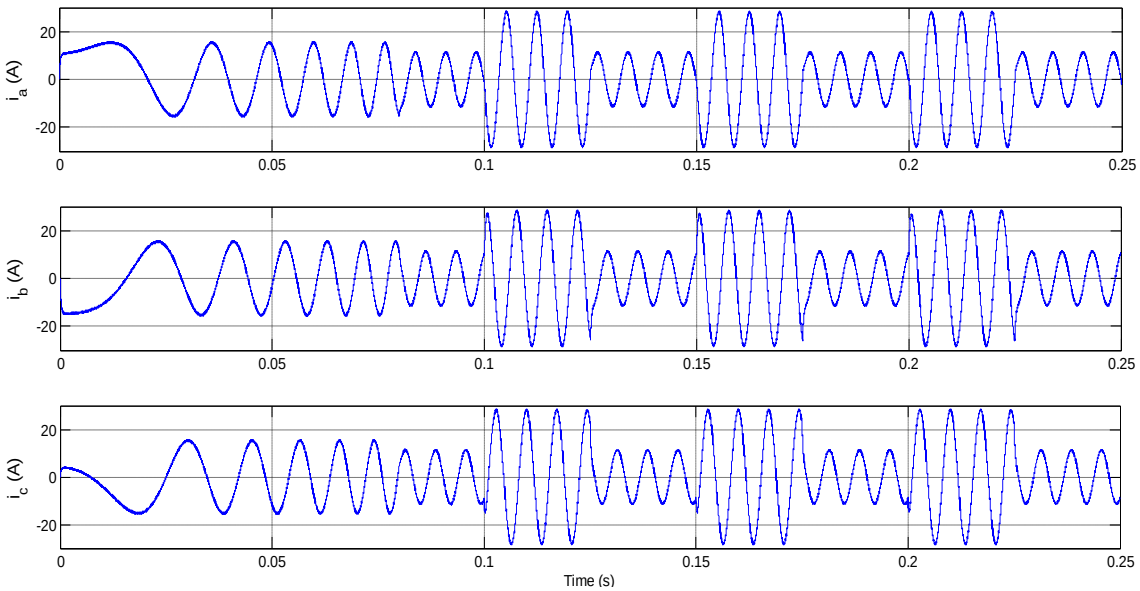

Fig. 3.11: Three-Phase Stator Currents

CHAPTER IV

PERFORMANCE RESULTS AND ANALYSIS

In this chapter, the results from simulations are presented and discussed. The operation of the proposed drive in steady state is first presented. Then the proposed drive is analyzed with respect to harmonics. All of the harmonic analysis is based on the steady state operation. Finally, the whole ac drive system is presented with a dynamic load. For the purpose of illustration and explanation, all simulation results presented from here on have a 20% input inductance and a command power factor of 0.94 lagging, unless otherwise stated.

4.1 Steady-State Behavior

To simulate the system in steady-state, the model shown in Fig. 3.4 of Chapter III was used. The load is a current source drawing FLA of 15.2 A from the rectifier. The dc bus is regulated at 375 V and is assumed to be initially charged to that voltage at the start of simulation. The resulting three-phase source currents are shown in Fig. 4.1. Fig. 4.2 shows a more detailed plot of the phase *a* source current and its corresponding reference waveform. The regulated dc bus voltage is shown in Fig. 4.3.

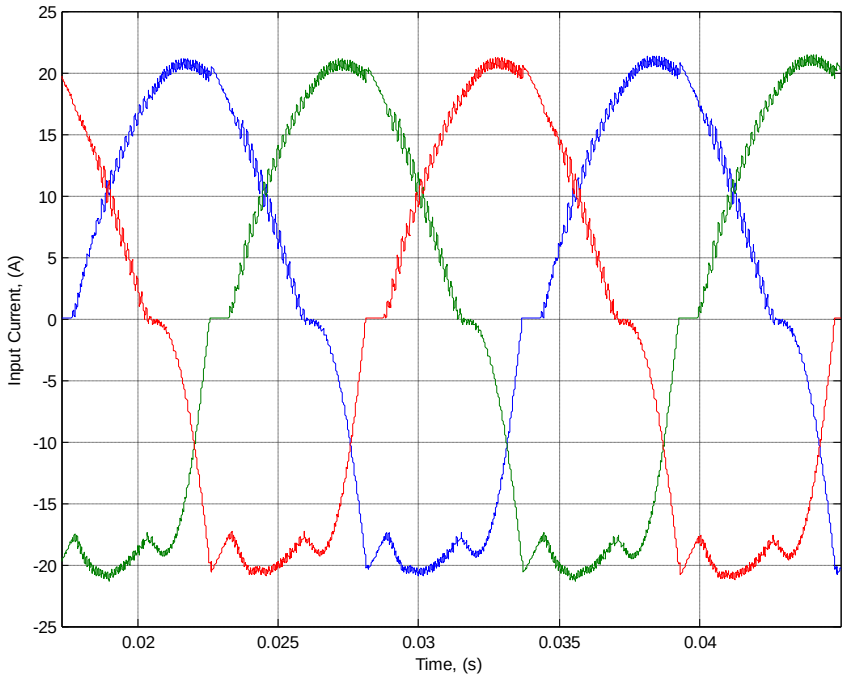

Fig. 4.1: Three-Phase Steady-State Source Currents

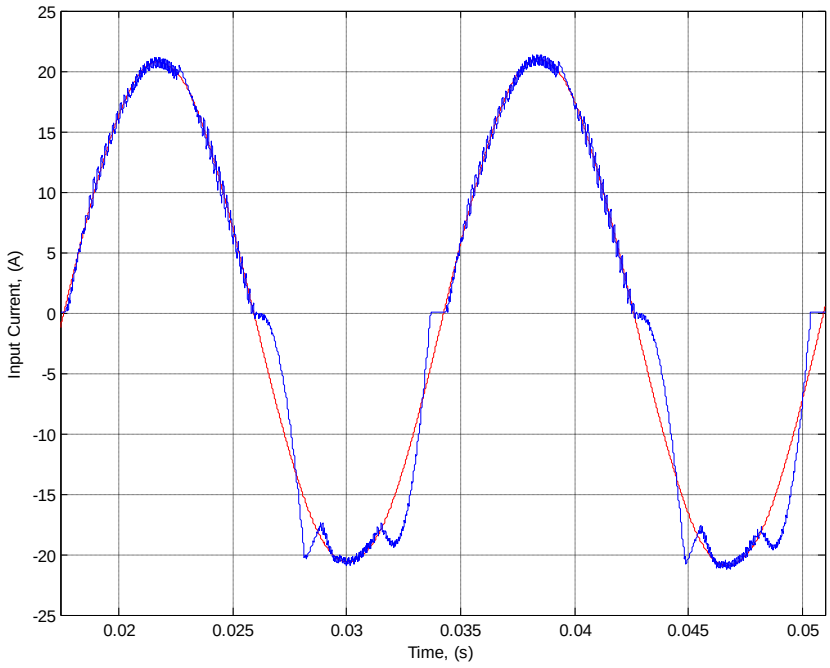

Fig. 4.2: Steady-State Phase A Input Current (blue) and Input Current Reference (red)

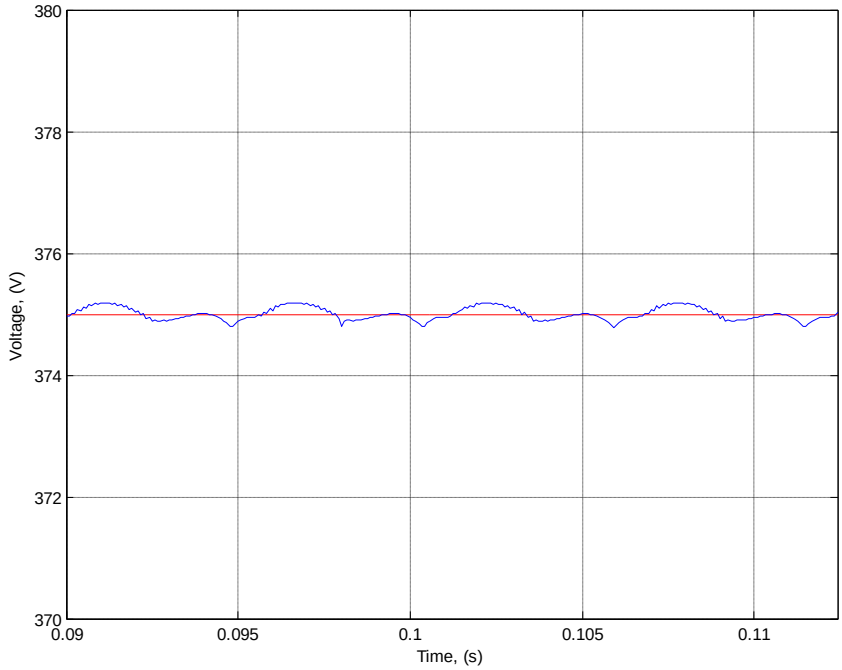

Fig. 4.3: Steady-State DC Bus Voltage Regulated at 375 V

Figs. 4.1 and 4.2 illustrate the ability of the proposed topology to shape the input currents. As mentioned in Chapter III, the positive half-cycles of the current waveforms are fully controlled as in a PWM rectifier. However, there are two regions in the negative half-cycle where the control is lost due to the passive anti-parallel diodes in the conduction paths.

After initial simulations, an adjustment was made to reset the current-loop PI controllers after each zero crossing. The integral term accumulates large errors during the uncontrolled regions which lead to a sluggish response once the control transitions to the fully controlled positive half-cycle regions.

4.2 Harmonic Analysis

The harmonics associated with this proposed ac drive are at the heart of this thesis. As shown in Fig. 4.1 and Fig. 4.2, the current waveforms contain asymmetries between the positive and negative half-cycles. This results in the generation of even multiple harmonics which can be detrimental to the power system. As will be shown throughout this section, the harmonics produced are largely dependent on the amount of input inductance used and also the desired power factor. However, even with optimal parameters selected, the even harmonics cannot be completely eliminated, as shown in Fig. 4.4 below.

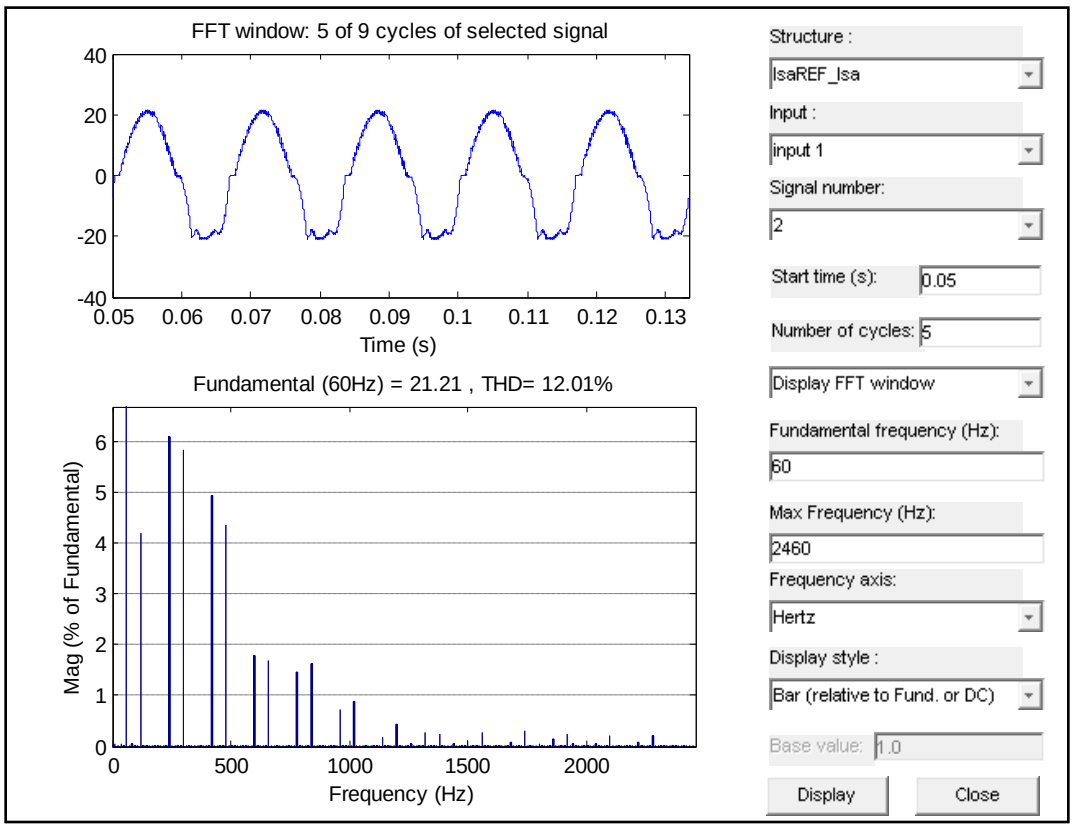

Fig. 4.4: Harmonic Spectrum of Input Current

Fig. 4.4 shows that the characteristic input current harmonic multiples are $3h \pm 1$. The waveforms contain significant amounts of odd and even multiples with the exception of the triplen (h = 3,6,9,…) harmonics.

One important key to note is that there is no dc component. The reason even harmonics are strictly governed is their implication of a dc offset. However, initial results suggest otherwise within the rectifier. Even harmonics can still produce an offset in power system transformers by the asymmetric transversal of the B-H curve, as discussed in Section 2.5.3. However, upon inspection, the positive and negative peaks of the current waveforms are approximately equal, preventing that from being the case.

The factors that have the greatest impact on the waveform quality are input inductance and commanded power factor. Fig. 4.5 and Fig. 4.6 illustrate the way that these factors affect the THD of the input current. The two graphs support the findings of Kikuchi [21]. The input current quality can be significantly improved by intentionally commanding a lagging power factor. With a 20% input reactor, the THD can be improved from 24.5% to 12% by commanding a 0.94 power factor rather than a unity power factor. And most utility systems require a 0.95 power factor or better.

Although the THD is significantly reduced compared to that of a three-phase diode bridge, the term THD gives no insight as to what harmonic multiples comprise the total distortion. The power quality indices TOHD and TEHD, as discussed in Section 2.5.6, are very useful measurements for analyzing the harmonic performance of the proposed drive. The harmonics produced are separated into even and odd harmonic components, and shown in Fig. 4.7 and Fig. 4.8.

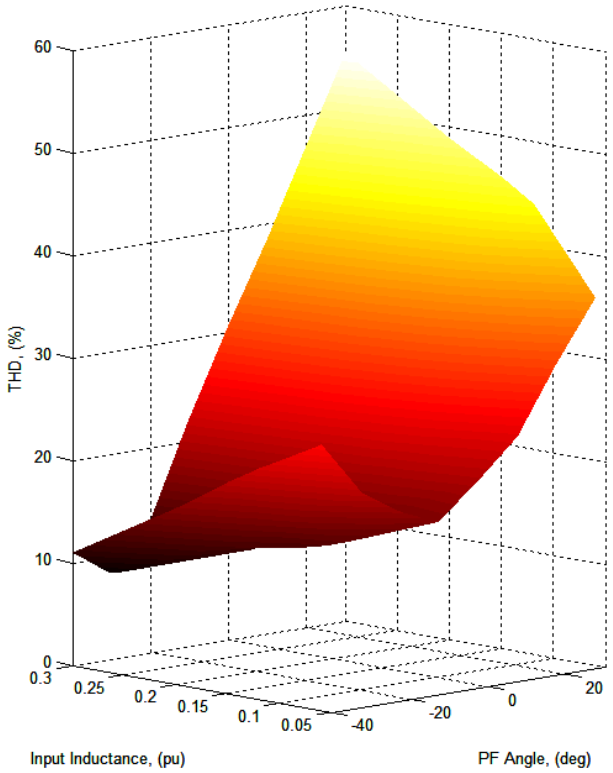

Fig. 4.5: Input Current THD

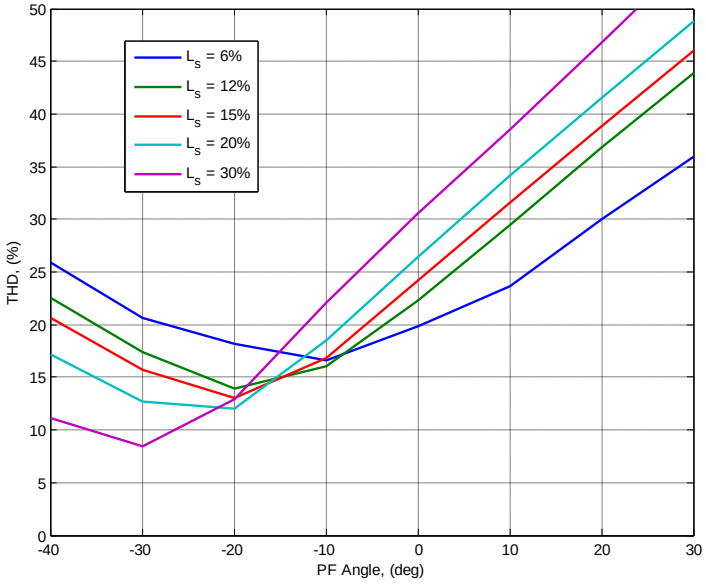

Fig. 4.6: Input Current THD vs. PF Angle

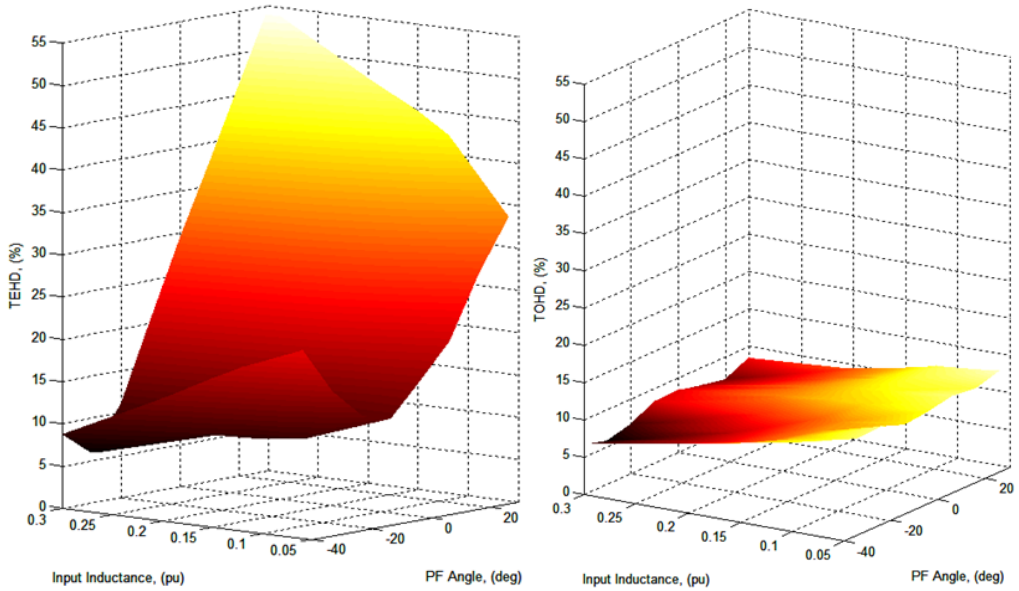

Fig. 4.7: Separation of Even and Odd Harmonic Components: (left) TEHD (right) TOHD

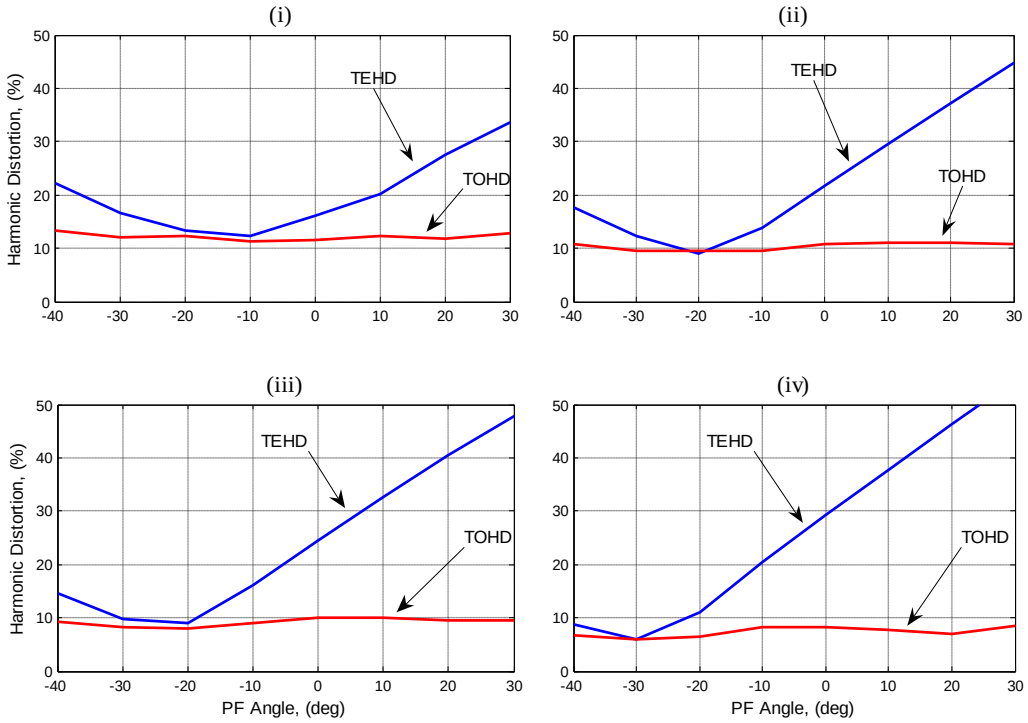

Fig. 4.8: Separation of Even and Odd Harmonic Components: (i) Ls=6% (ii) Ls=15% (iii) Ls=20% (iv) Ls=30%

It is interesting to note the sensitivity of the two types of harmonics. The TOHD remains almost constant throughout the changing power factor parameter, but is sensitive to the amount of input inductance. The TEHD on the other hand, is much more sensitive, mostly to the commanded power factor. It has been shown that even harmonics arise from asymmetries. Upon inspecting Fig. 4.9(i), (ii), and (iii), the progressively increasing symmetry from a 0.94 leading power factor to a 0.94 lagging power factor is obvious, which results in a lower amount of even harmonics.

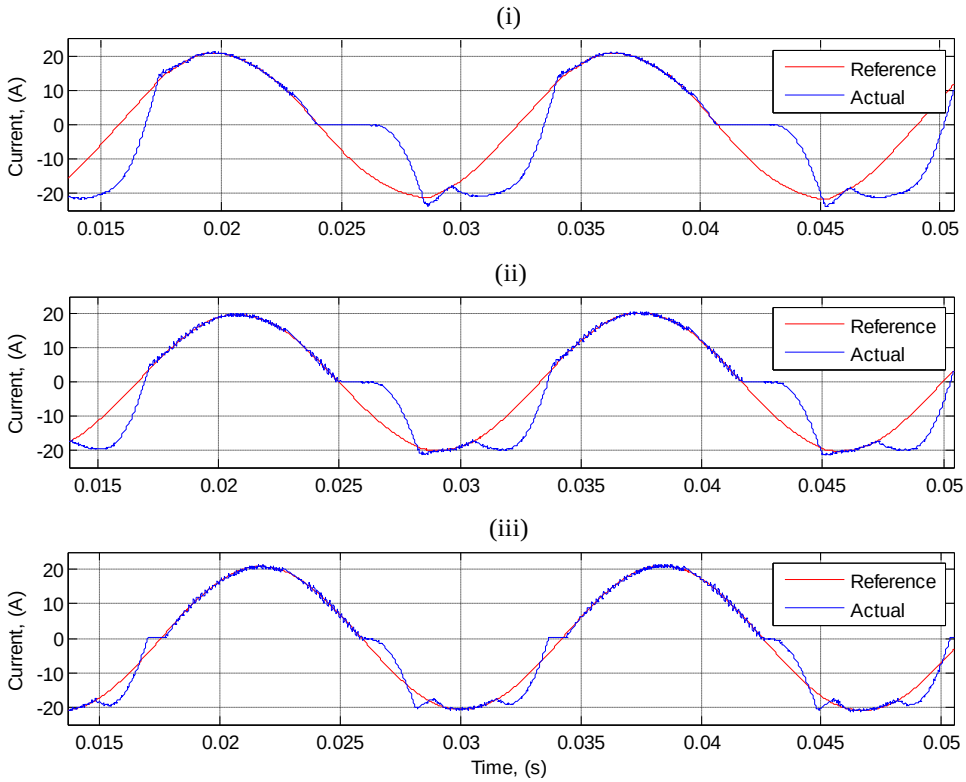

Fig. 4.9: Comparison of Different Power Factor Commands with 20% Input Inductance: (i) 0.94 leading (ii) Unity (iii) 0.94 lagging

4.3 Transient Behavior

It is also important to model the entire system with an accurate load and see how it behaves. The inverter-fed PMSM discussed in Section 3.3.4 is used as a load to the rectifier being considered (see Fig. 4.10). First the dc bus voltage is precharged to 375 V before the load is engaged. After the bus voltage has reached the desired value, the PMSM is brought up to the desired speed of 220 rad/s and satisfies a fluctuating load torque while holding its constant speed. The PMSM fluctuates between full power and half power. This dynamic loading, and its effect on the rest of the ac drive system, is given in Fig. 4.11, Fig. 4.12, and Fig. 4.13.

Fig. 4.11(i) shows the speed response of the PMSM. The acceleration of the PMSM is limited only by the magnitude of quadrature current, which is limited to 40 A by the controller. Fig. 4.11(ii) and (iii) show the quadrature axis current and direct axis current, respectively. Since the direct axis current is commanded to be zero, the quadrature axis current is directly proportional to the torque. Therefore, the torque plot resembles Fig. 4.11(ii). Fig. 4.12(i), (ii), and (iii) illustrate the currents output by the inverter from the stationary stator reference frame. Fig. 4.13(i) and (ii) illustrate the dc bus voltage and input source currents from the utility. As shown in the graphs, the dc bus has some ripple. In fact, the amount of ripple is a tradeoff with the quality of input current. The dc bus controller can response more rapidly, however, it creates significant distortion in the input current waveforms.

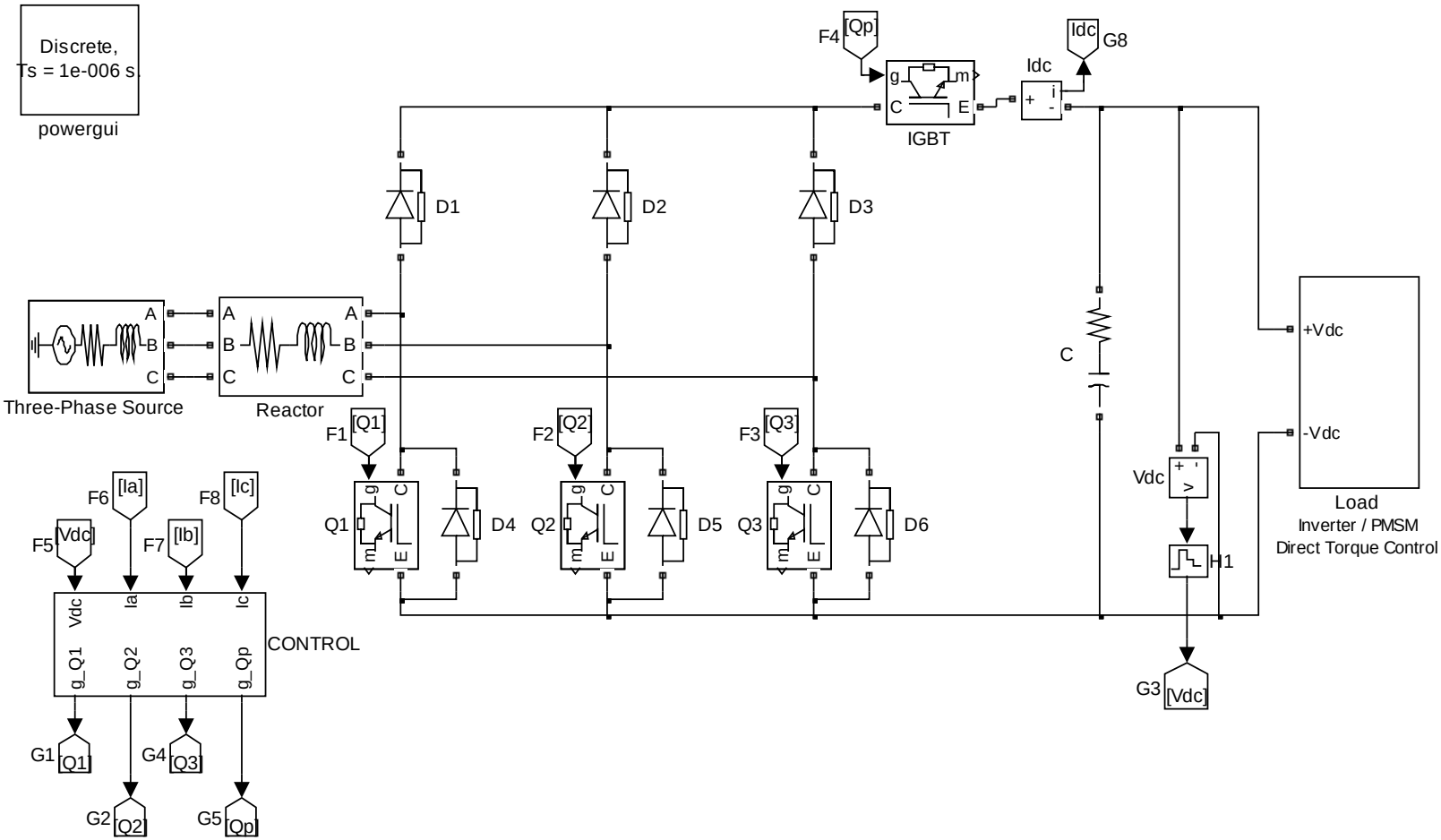

Fig. 4.10: Transient Simulation Model

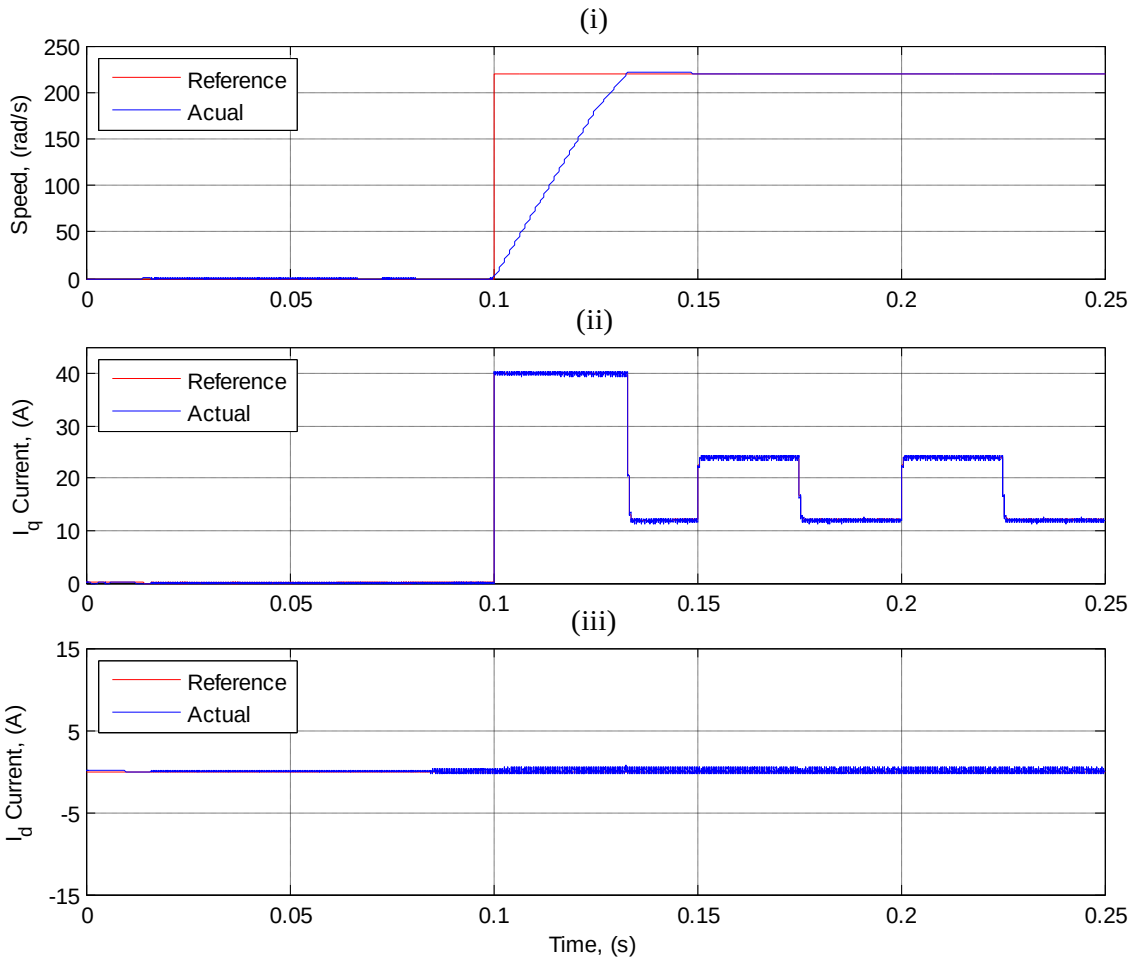

Fig. 4.11: Transient Response of PMSM: (i) Speed response (ii) Quadrature axis current (iii) Direct axis current

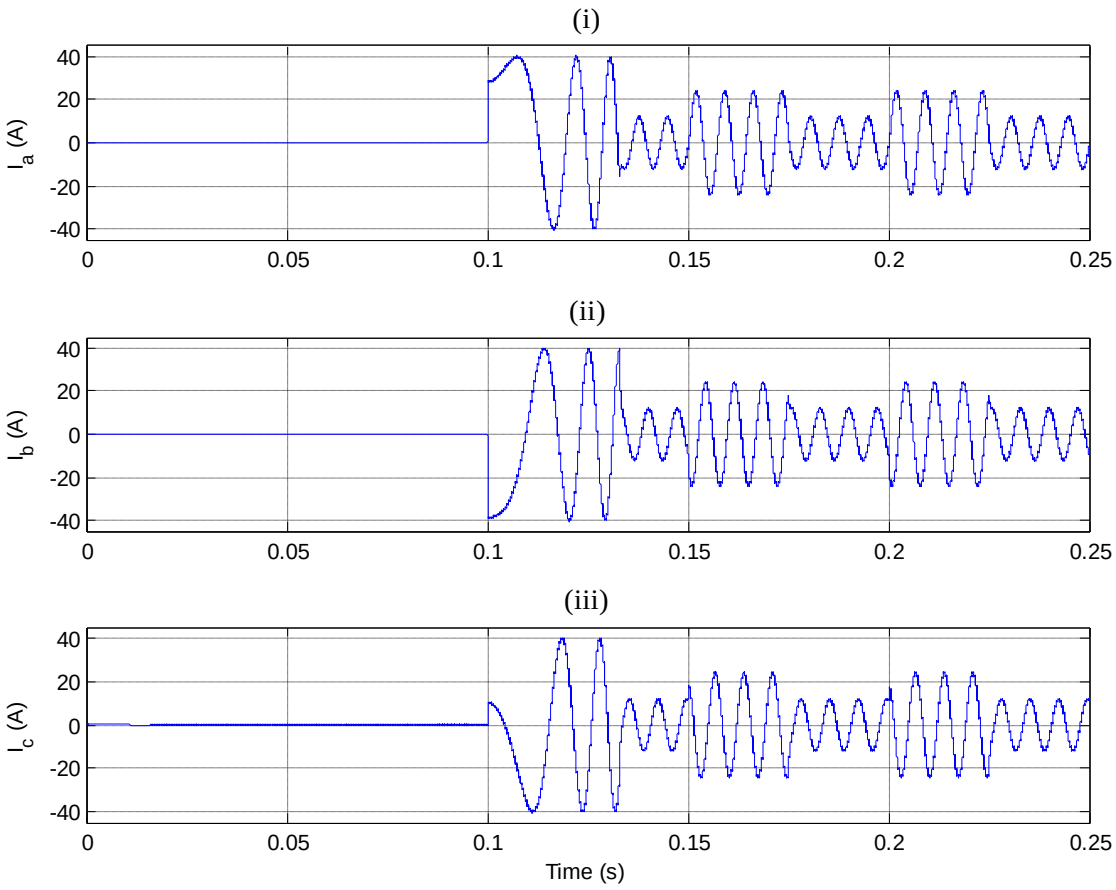

Fig. 4.12: Transient Response of Inverter: (i) Phase A (ii) Phase B (iii) Phase C

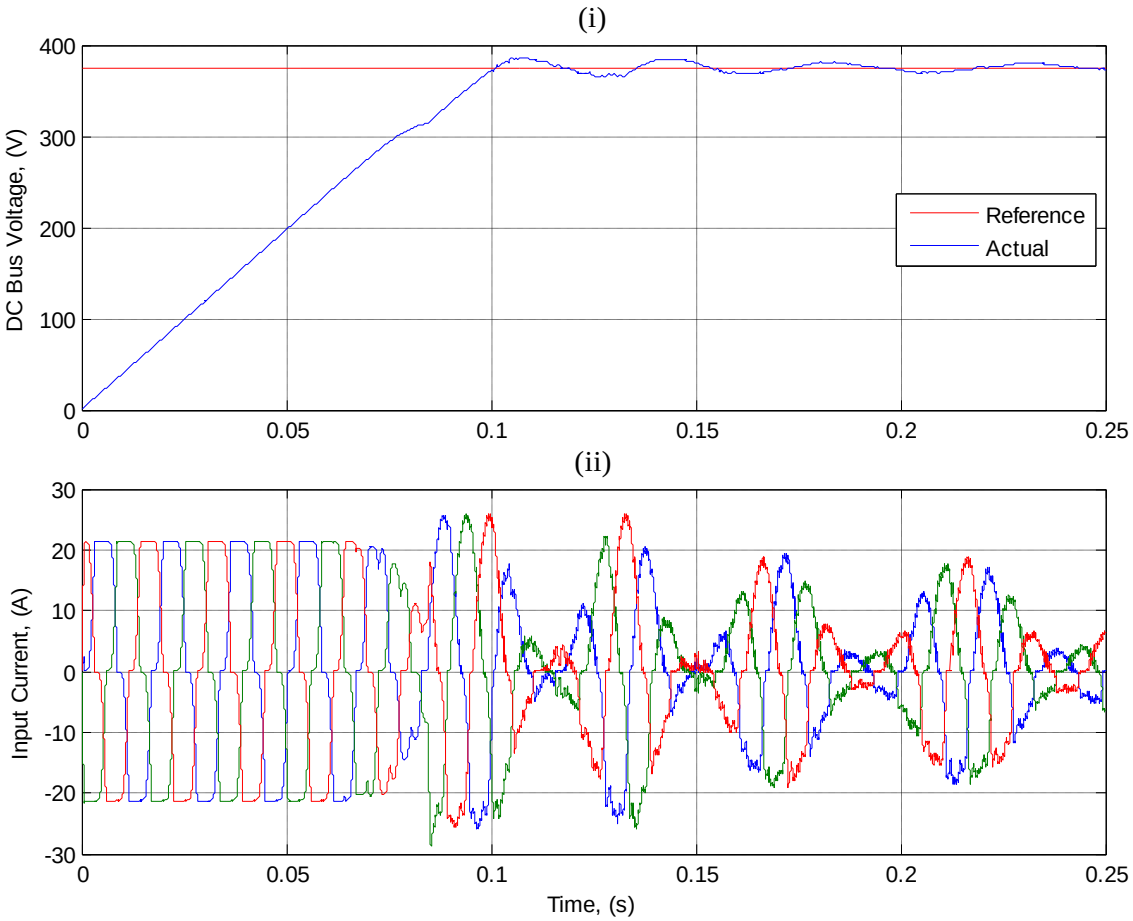

Fig. 4.13: Transient Response of Rectifier: (i) DC bus voltage (ii) Three-phase input currents

The change in slope of the bus voltage in Fig. 4.13(i) represents the transition from passive rectification to the boosting action of the rectifier. In Fig. 4.13(ii), the first mode of operation lasts until about 0.08 s and is the constant current precharge. Next, the PMSM is commanded to speed up and thus the rectifier must supply large currents to the dc link. Finally, the current pulsates to satisfy the pulsating load requirements of the PMSM.

CHAPTER V

CONCLUSION AND RECOMMENDATIONS

In this chapter the thesis will be concluded. An overview of the advantages and disadvantages of the proposed ac drive topology will be given. Also, a recommendation will be given as to whether or not this topology should be pursued in industry.

5.1 Conclusions

It has been shown that the proposed ac drive topology has several advantages, as well as disadvantages. The drive offers a reduced parts count and a reduced cost compared to a PWM rectifier. This topology requires that only three active switches are utilized. Furthermore, only one isolated power supply is used, rather than four with the PWM rectifier. Yet, the drive is still capable of controlling the dc bus voltage and regulating the power factor.

In terms of THD, the drive significantly out performs a diode bridge rectifier. Typical diode rectifiers produce around 45% THD in the input current. It was shown in Chapter IV that the proposed drive can reduce the THD to 12%. However, the use of THD as the prominent power quality index is a poor choice. Therefore, the THD should be separated into even and odd components, resulting in the use of TEHD and TOHD as the prominent power quality indices. Considering TEHD and TOHD, the performance of the proposed drive becomes less attractive. The harmonics produced in the input current contain significant amounts of even multiple frequencies. Furthermore, it was also

shown that these even harmonics are very sensitive to the commanded power factor and the 12% THD mentioned above is a best case scenario. The odd harmonics, on the other hand, are significantly less sensitive than their even counterparts, and depend mostly on the amount of input inductance and not the commanded power factor.

5.2 Recommendations

Even harmonics are detrimental to the integrity of the power system and IEEE imposes very strict standards on the acceptable levels of even harmonics. The IEEE-519-1992 Standard limits even harmonics to one-fourth the level allowed for odd harmonics, and allows an overall THD level of no more than 5.0%. Thus, with the compliance of the IEEE Standards becoming one of the most important design features of a drive, it is not recommended to pursue this topology in industry.

The even harmonics arise from the waveform asymmetries that are produced because the rectifier cannot control the current in portions of the negative half-cycle of current. The lack of control is a result of passive diode commutation in the lower legs of each phase. The only way to prevent this phenomenon is to have at least one controlled element in the negative half-cycle conduction path, which would indicate the use of more switches and approach the complexity and part count of a conventional PWM rectifier.

REFERENCES

[1] "AC Drives Market Will Be Worth More Than $16B by 2011," *World News*: June 2007, Accessed: Aug. 20, 2007, [online] Available: www.drives.co.uk/fullstory.asp?id=2022

[2] Western Area Power Administration, *Technical Brief: Energy Efficient Motors*, Accessed: Aug 18, 2007, [online] Available: www.wapa.gov/es/pubs/techbrf/eemotors.htm.

[3] Energy Information Administration, *Annual Energy Review 2006*, location: U.S. Department of Energy, June 2007.

[4] Energy Information Administration, *Total Electric Power Industry Summary Statistics*, location: U.S. Department of Energy, August 2007.

[5] N. Mohan, *Electric Drives: An Integrated Approach*, Minneapolis, MN, MNPERE, 2003.

[6] F. Aart, "Energy Efficiency in Power Plants," *In Proc. Integrated Pollution Prevention and Control Conference*, Vienna, Austria, Oct. 21, 2004.

[7] Washington State University Cooperative Extension Energy Program, *Adjustable Speed Motor Drives: Energy Efficiency Factsheet*, Accessed: Aug 21, 2007, [online] Available: www.energy.wsu.edu/documents/engineering/motors/MotorDrvs.pdf

[8] G. L. Stark, *Adjustable Speed Drives*, Lecture slides for AGSM 325 course, Texas A&M University, April 27, 2007. [online] Available: www.baen.tamu.edu/users/stark/AGSM325_files/Lecture/8%20ASD%20Lecture.325.pdf

[9] I. Ashida, J. Itoh, "A Novel Three-Phase PFC Rectifier Using a Harmonic Current Injection Method," *In Proc. Power Conversion Conference, Nagoya, 2007*, April 2-5, 2007 pp. 1302-1307.

[10] H. H. Moghbelli, M. H. Rashid, "Performance Review of AC Adjustable Drives," Industrial Electronics Society, 1990, *16th Annual Conference of IEEE*, Nov. 27-30, 1990, pp. 895-902, vol. 2, Pacific Grove, CA.

[11] H. A. Toliyat, S. G. Cambell, *DSP-Based Electromechanical Motion Control*, Boca Raton, FL: CRC Press. 2003.

[12] D. W. Novotny, T. A. Lipo, *Vector Control and Dynamics of AC Drives*, Oxford University Press, Oxford, England, 2005.

[13] G. J. Wakileh, *Power Systems Harmonics: Fundamentals, Analysis, and Filter Design*, New York: Springer. 2001.

[14] F. C. De La Rosa, *Harmonics and Power Systems*, New York: Electronic copy, Taylor and Francis. 2006.

[15] IEEE Recommended Practices and Requirements for Harmonic Control in Electrical Power Systems, IEEE 519, 1992.

[16] Y. Liu and G. T. Heydt, "Power System Even Harmonics and Power Quality Indices," in *Electric Power Components and Systems*, New York: Taylor and Francis, 2005, pp. 833-844.

[17] Halpin, S. M. "Comparison of IEEE and IEC Harmonic Standards." *In Proc. IEEE Power Engineering Society General Meeting.* IEEE, 2005, pp. 2214-2216.

[18] A. Emadi, A. Nasiri, S. Bekiarov, *Uninterruptible Power Supplies and Active Filters*, New York: CRC Press, 2005.

[19] Mark McGranaghan, *Active Filter Design and Specification for Control of Harmonics in Industrial and Commercial Facilities*, Knoxville, TN: Electrotek Concepts, Inc.

[20] J. Kikuchi, M. Manjrekar, T. Lipo, "Performance Improvement of Half Controlled Three Phase PWM Boost Rectifier," *In Proc. IEEE Power Electronics Specialists Conference*, Charleston, SC, Aug. 1999, Vol 1, pp. 319-324.

APPENDIX A

PARAMETER DEFINITIONS M-FILE

```
% Active Filter Non-Regen AC Drive Research
% Baldor Electric Co. / Texas A&M University
% Power Electronics and Motor Drives Laboratory
% Prepared by: Alex Skorcz
% July 3, 2007

% You must execute this m-file first to define the variables
% that will be used in the SIMULINK simulation

clear
clc

% Choose Percent inductance (Lbase = 24.18 mH)
    %Laf = 1.45e-3;   % 6% inductance
    %Laf = 2.90e-3;   % 12% inductance
    %Laf = 3.63e-3;   % 15% inductance
    Laf = 4.84e-3;   % 20% inductance
    %Laf = 7.25e-3;   % 30% inductance
    %Laf = 9.67e-3;   % 40% inductance

% Set desired switching frequency in Hz
fs = 12000;

% Choose desired power factor angle in degrees
% (Negative for Lagging)
PFangle = -20;

% DC Bus Capacitance
C = 5400e-6;

% DC Bus Command Voltage
Vdc_REF = 375;

                          % Rectifier Control
%%%%%%%%%%%%%%%%%%%%%%%%%%%%%%%%%%%%%%%%%%%%%%%%%%%%%%%%%%%%%%%%%%%%%%%%%%%%
% Kp and Ki gains for Current-Loop PI controllers
Kp_I = 0.4;
Ki_I = 1000;

% Kp and Ki gains for Voltage-Loop PI controller
Kp_Vdc = 0.004;
Ki_Vdc = 1;

                            % PMSM Control
%%%%%%%%%%%%%%%%%%%%%%%%%%%%%%%%%%%%%%%%%%%%%%%%%%%%%%%%%%%%%%%%%%%%%%%%%%%%
% Kp and Ki gains for Iq Controller
Kp_Iq = 500;
Ki_Iq = 1000;

% Kp and Ki gains for Id Controller
Kp_Id = 450;
Ki_Id = 15000;

% Kp and Ki gains for torque Controller
Kp_T = 5.8;
Ki_T = 60000;

% Kp and Ki gains for speed Controller
Kp_W = 25;
Ki_W = 1000;

%%%%%%%%%%%%%%%%%%%%%%%%%%%%%%%%%%%%%%%%%%%%%%%%%%%%%%%%%%%%%%%%%%%%%%%%%%%%
```

APPENDIX B

STEADY-STATE MODEL IMPLEMENTED IN SIMULINK

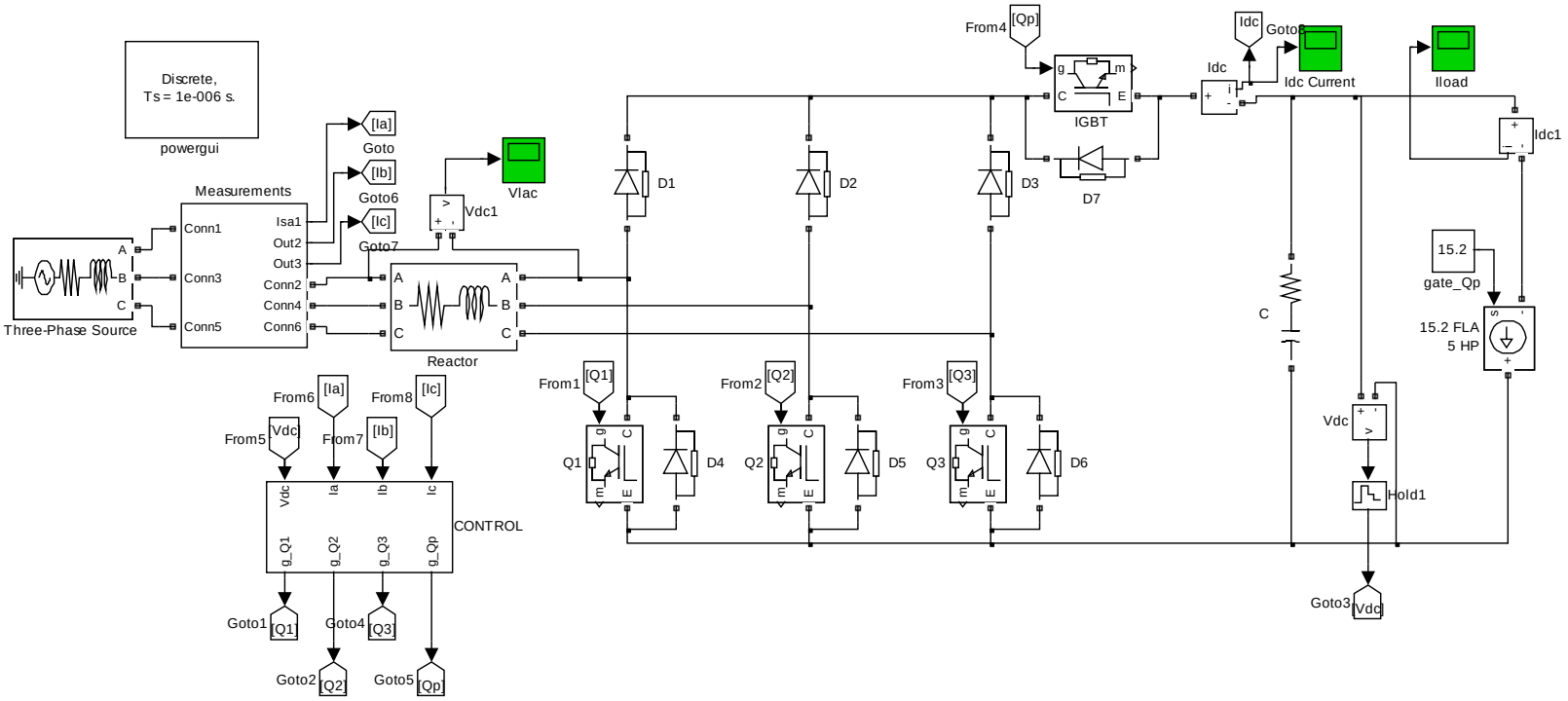

Fig. B.1: Steady-State Model

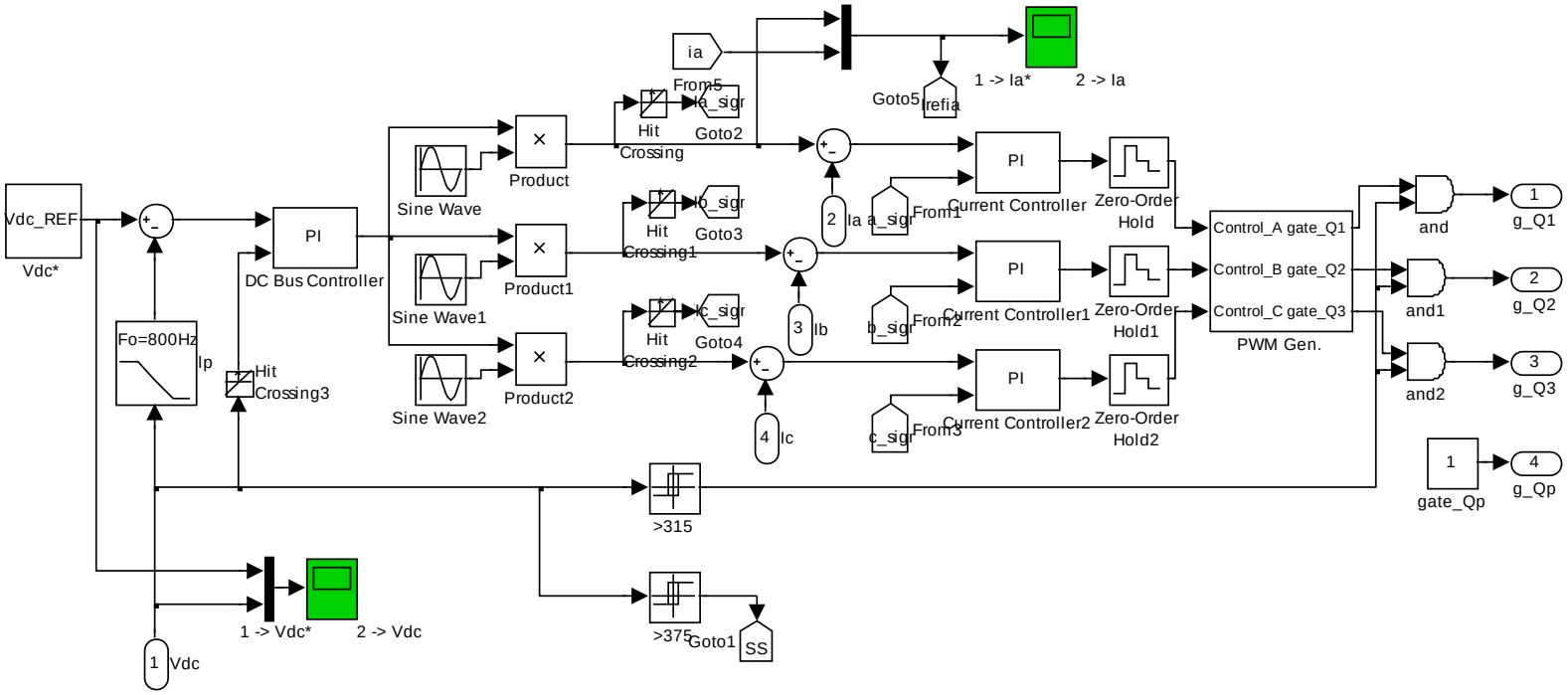

Figure B.2: Steady-State Control Subsystem

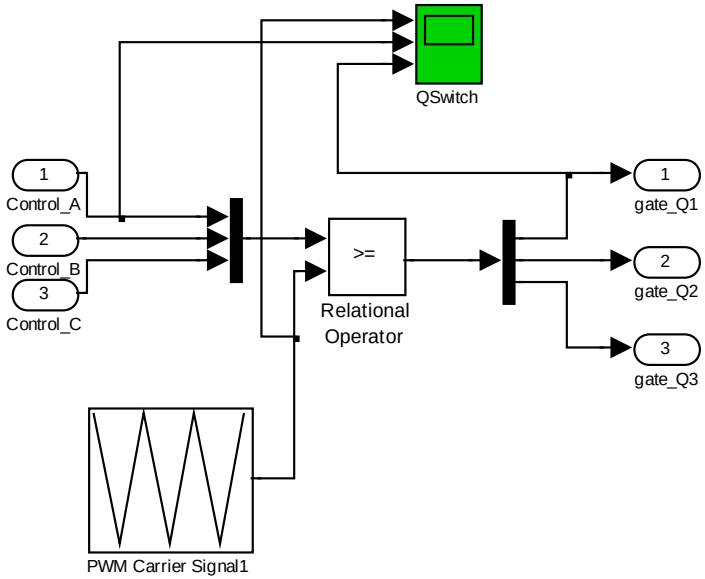

Figure B.3: PWM Generator Subsystem

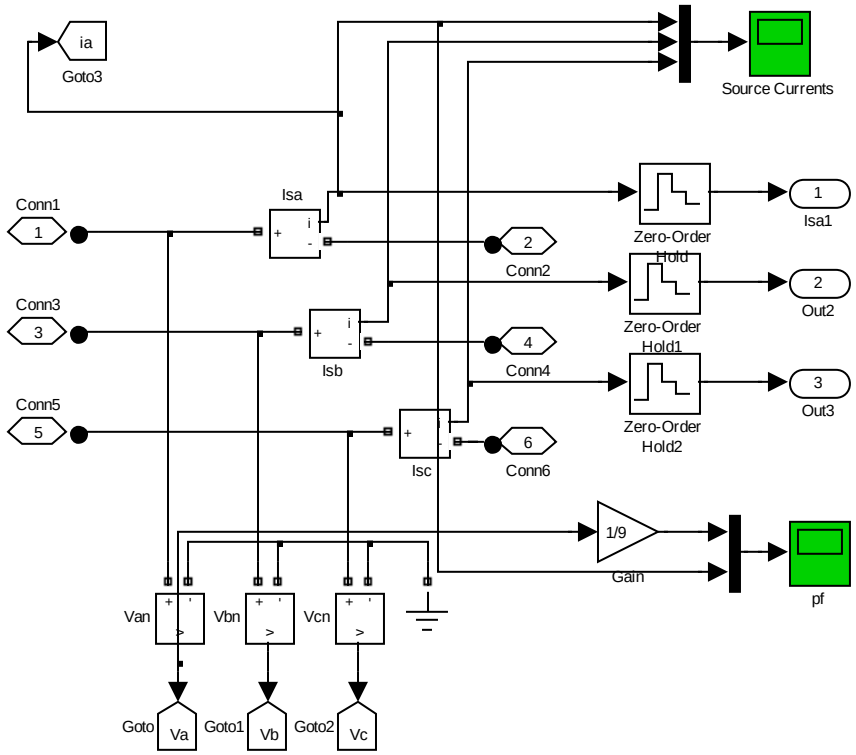

Figure B.4: Measurements Subsystem

APPENDIX C

TRANSIENT SIMULATION MODEL IMPLEMENTED IN SIMULINK

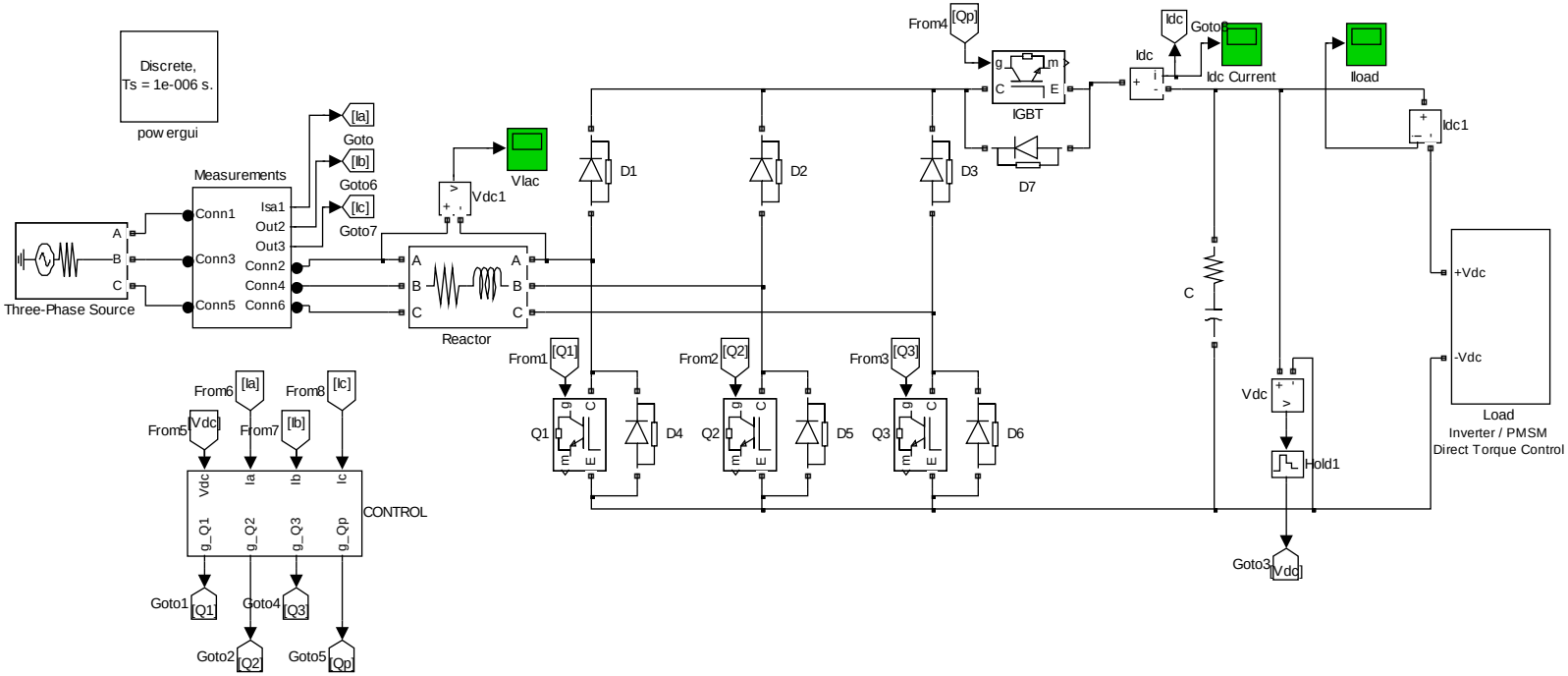

Fig. C.1: Transient Model

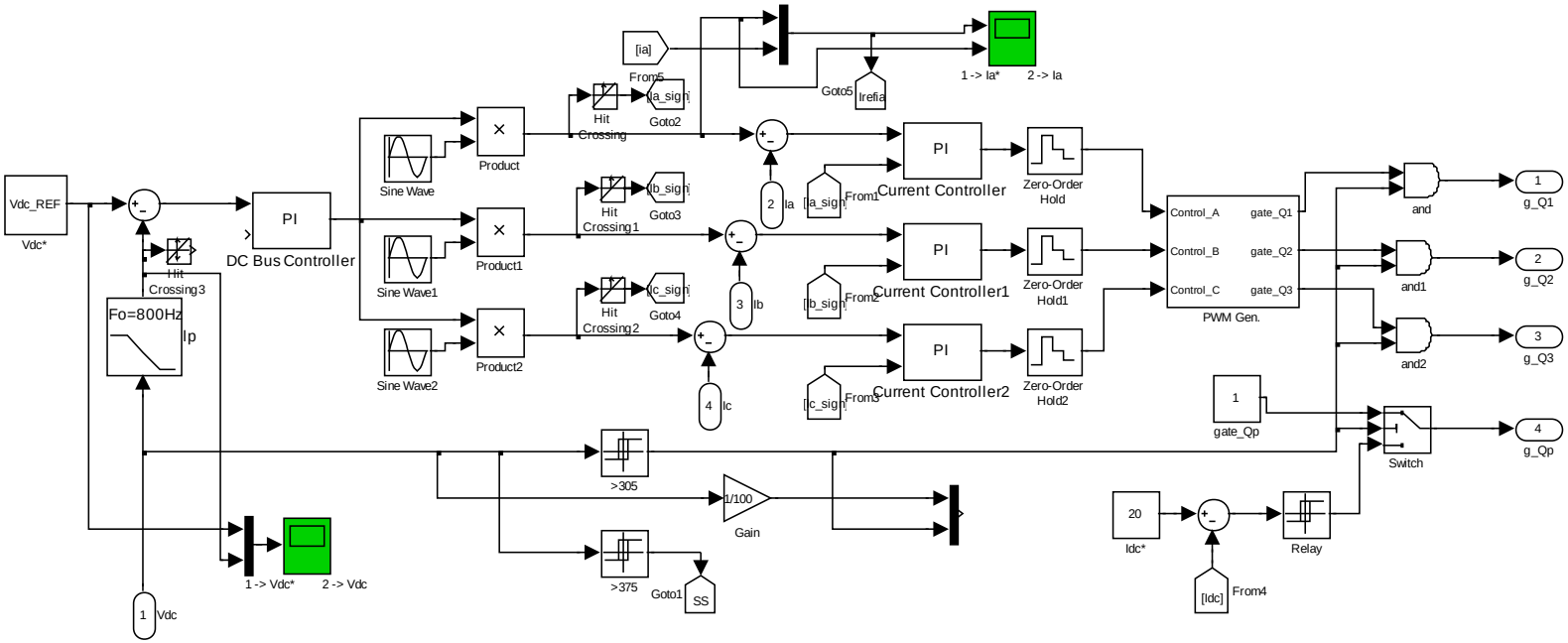

Fig. C.2: Transient Control Subsystem

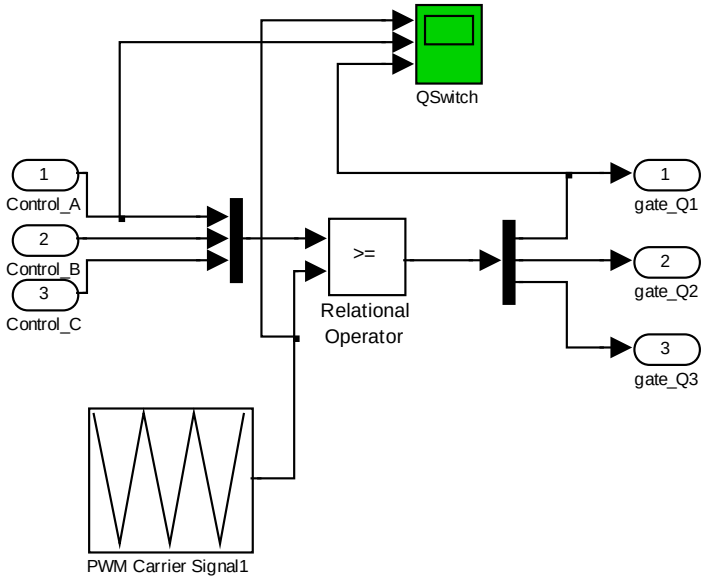

Fig. C.3: PWM Generator Subsystem

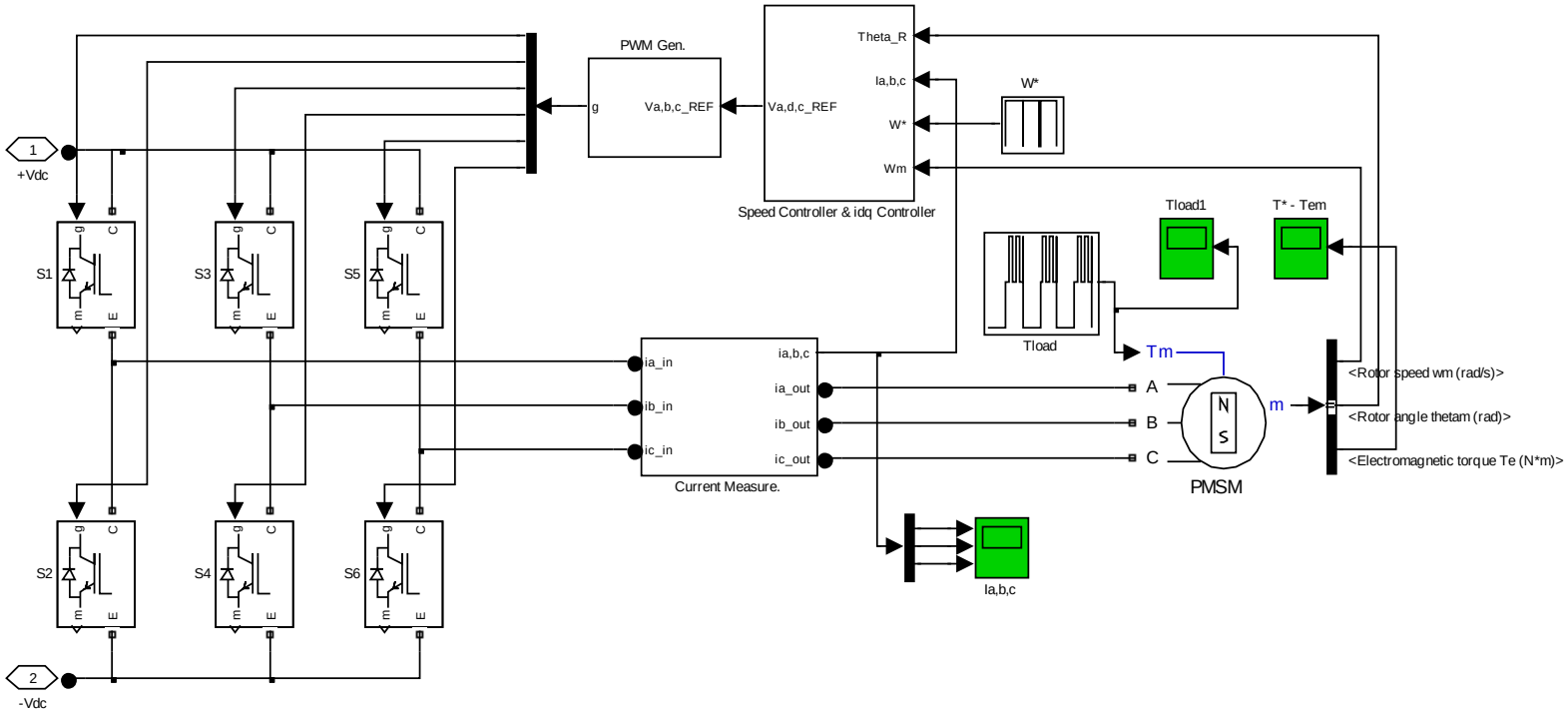

Fig. C.4: PMSM Load Model

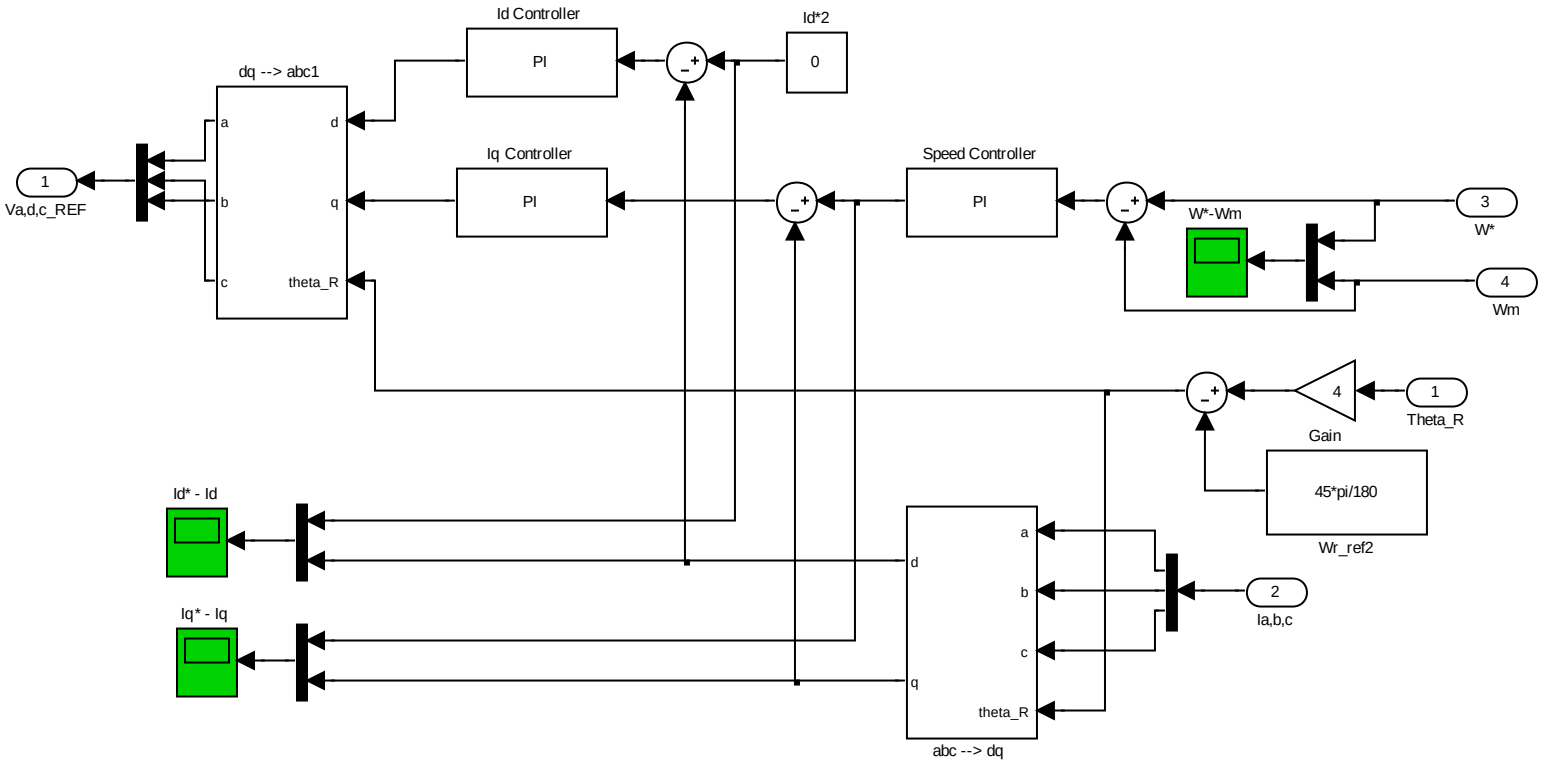

Fig. C.5: Speed and Torque Controller Subsystem

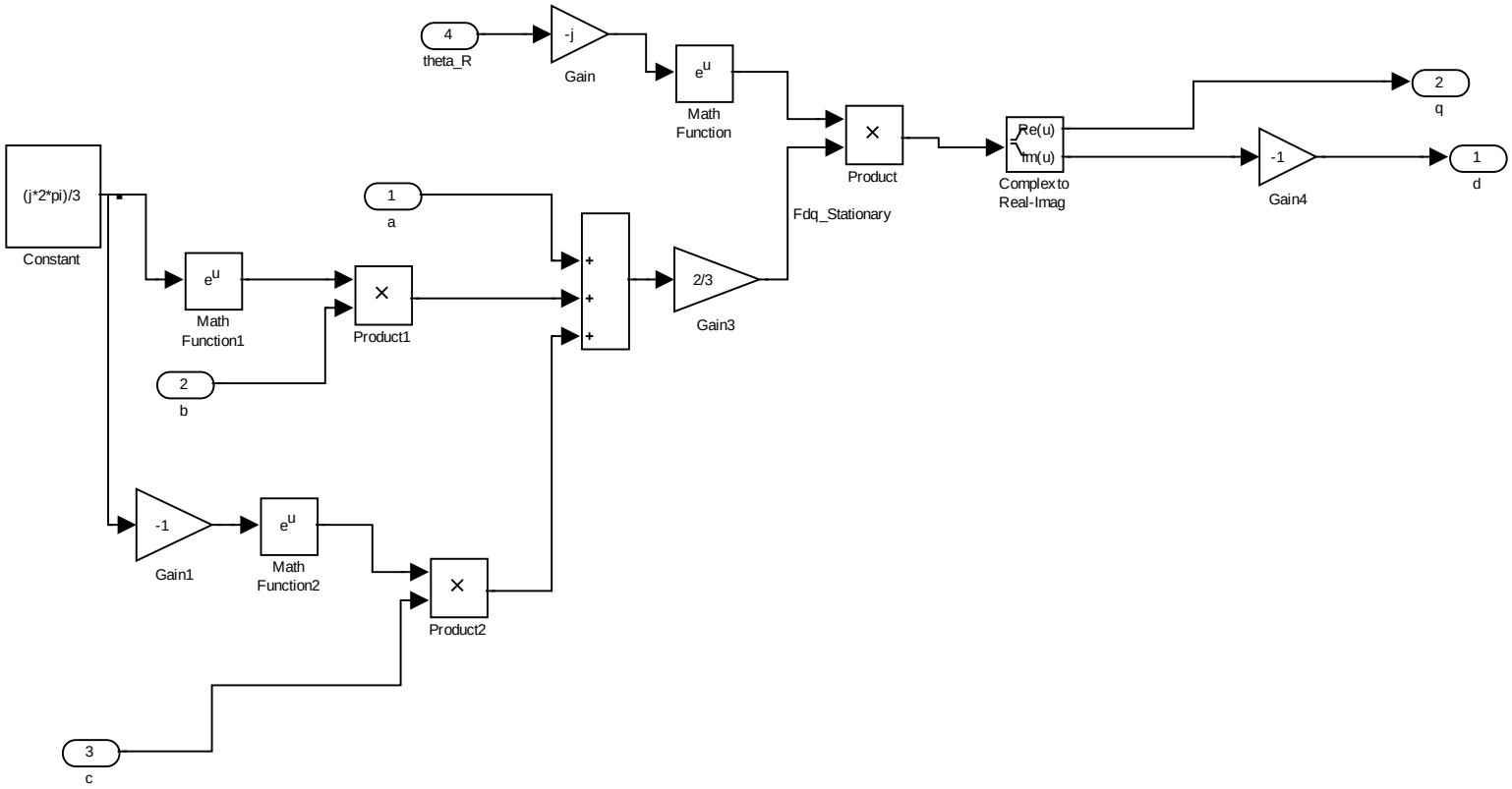

Fig. C.6: ABC to DQ Transformation Subsystem

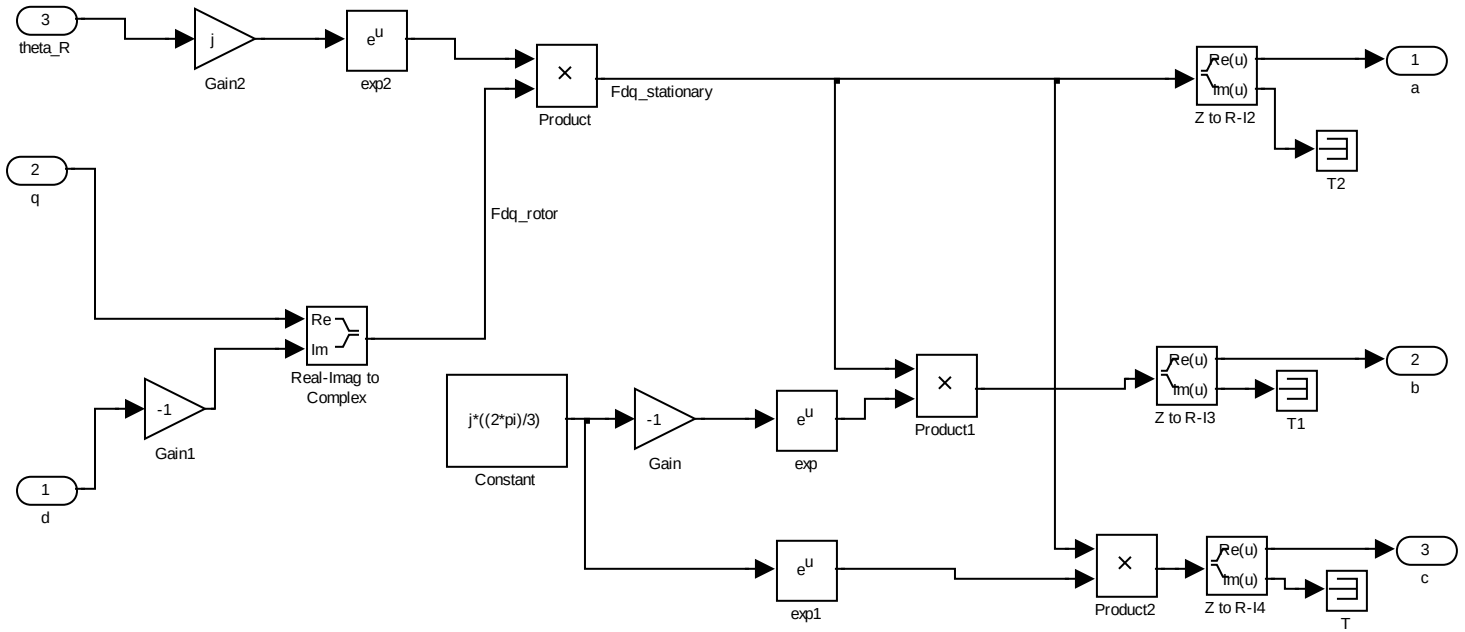

Fig. C.7: DQ to ABC Transformation Subsystem

APPENDIX D

HARMONIC DATA COLLECTED

Table D.1: Input Current Harmonic Components with L_s = 6%

	pf=+30	pf=+20	pf=+10	pf=0	pf=-10	pf=-20	pf=-30	pf=-40
THD	35.95	30.06	23.64	19.89	16.62	18.14	20.68	25.88
TEHD	33.58	27.60	20.22	16.15	12.29	13.25	16.73	22.22
TOHD	12.83	11.92	12.27	11.62	11.19	12.38	12.16	13.28
0	0.08	0.91	0.04	0.17	0.24	0.21	0.03	0.08
1	100	100	100	100	100	100	100	100
2	26.19	19.82	13.66	11.33	8.46	7.82	11.04	15.86
3	0.49	0.63	0.41	0.9	0.64	0.65	0.44	0.49
4	19.66	18.13	13.67	8.17	2.75	6.07	10.76	14.26
5	11.11	10.29	9.19	6.49	4.2	5.84	7.68	10.74
6	0.37	0.12	0.34	0.82	0.64	0.37	0.12	0.18
7	4.2	3.53	6.34	6.52	8.1	9.22	8.24	5.48
8	4.8	3.86	3.95	1.99	2.42	4.97	4.62	2.44
9	0.22	0.68	0.48	0.38	0.56	0.28	0.31	0.09
10	3.2	3.15	2.3	6.2	6.86	5.01	2.13	4.04
11	2.69	3.18	2.47	3.13	5.04	2.23	1.98	3
12	0.37	0.27	0.37	0.29	0.51	1.25	0.55	0.4
13	1.66	1.46	2.88	3.98	1.82	1.43	2.63	2.97
14	3.18	1.36	2.41	2.21	1.05	0.37	2.15	1.64
15	0.42	0.09	0.35	0.68	0.36	0.62	0.52	0.66
16	1.42	1.56	0.65	2.01	0.72	3.18	1.91	1.61
17	0.92	0.52	1.08	2.25	1.3	2.74	1.39	1.88
18	0.81	0.37	0.14	0.9	0.74	0.43	0.28	0.54
19	1.85	0.45	1.36	1.4	0.84	2.48	0.89	0.78
20	0.96	1.28	0.91	2.02	1.7	1.48	1.61	1.37
21	0.69	0.04	0.43	1.61	1.25	0.73	0.47	0.51
22	1.08	1.92	0.99	1.81	1.81	1.05	0.74	0.52
23	1.32	1.29	1.38	1.46	1.3	0.96	1.03	1.36
24	0.32	0.82	0.46	0.75	1.32	0.18	0.94	0.84
25	0.81	1.85	0.66	2.17	1.76	0.87	0.76	0.62
26	1.1	0.66	0.35	0.37	1.28	1.19	0.76	1.11
27	0.32	1.24	0.62	0.83	0.87	0.57	0.74	0.47
28	0.65	0.82	1.01	1.39	0.31	2.19	0.82	0.66
29	0.58	0.33	1.59	0.73	0.47	1.74	1.43	0.89
30	1.18	0.63	0.7	0.28	1.02	0.56	0.09	1.12
31	0.84	0.44	0.44	1.32	1.42	2.17	0.91	1.18
32	1.16	0.39	1.6	0.91	0.22	1.27	0.24	1.27
33	0.99	1.16	1.2	0.81	0.18	0.27	0.15	1.04
34	0.11	0.46	0.07	0.49	1.69	1.87	0.68	0.65
35	1.63	0.89	0.2	1.24	0.13	0.43	0.33	0.5
36	0.42	0.33	1.05	0.15	0.37	0.15	0.3	0.83
37	0.74	0.52	0.78	1.2	0.6	1.43	0.92	0.92
38	1.08	1.42	0.35	1.16	1.36	0.86	0.93	1.2
39	0.8	0.93	0.37	0.42	0.5	0.32	0.72	1.11
40	1.03	0.87	0.62	0.63	0.8	0.2	0.88	0.84

Table D.2: Input Current Harmonic Components with L_s = 12%

	pf=+30	pf=+20	pf=+10	pf=0	pf=-10	pf=-20	pf=-30	pf=-40
THD	43.93	36.81	29.52	22.29	16.01	13.97	17.35	22.53
TEHD	42.27	34.86	27.21	19.39	12.36	9.58	13.67	19.42
TOHD	11.97	11.79	11.44	11.00	10.17	10.16	10.68	11.42
0	0	0.11	0.05	0.02	0.03	0.14	0.06	0.09
1	100	100	100	100	100	100	100	100
2	38.18	29.99	21.94	14.37	8.21	4.35	9.52	14.79
3	0.15	0.15	0.19	0.14	0.07	0.08	0.11	0.06
4	16.89	16.82	15.38	12.42	7.26	5.27	8.32	11.82
5	9.11	10.45	10.61	9.66	7.37	6.79	8.33	9.63
6	0.15	0.06	0.14	0.19	0.11	0.21	0.23	0.14
7	7.12	4.79	3.29	4.26	5.83	6.66	6.14	5.47
8	6.14	5.09	3.4	3.2	4.19	5.15	4.16	3.36
9	0.17	0.2	0.07	0.15	0.16	0.3	0.09	0.04
10	1.81	2.07	2.61	1.02	2.98	3.58	2.3	1.63
11	2.73	1.81	2.05	1.95	2.78	2.62	1.72	1.65
12	0.17	0.19	0.18	0.13	0.07	0.19	0.06	0.1
13	0.39	1.36	0.27	1.53	1.81	0.86	1.18	1.78
14	1.17	1.2	0.99	1.14	1.43	0.95	1.07	1.69
15	0.13	0.04	0.17	0.18	0.08	0.01	0.15	0.1
16	0.68	0.63	0.62	0.73	1.33	0.23	0.83	0.53
17	0.9	0.79	0.78	0.93	1.15	0.53	1.12	0.56
18	0.08	0.22	0.13	0.07	0.17	0.1	0.08	0.2
19	0.64	0.17	0.05	0.53	0.49	0.63	0.43	0.28
20	0.84	0.65	0.32	0.7	0.68	0.31	0.84	0.84
21	0.11	0.34	0.2	0.27	0.15	0.13	0.13	0.42
22	0.3	0.08	0.85	0.28	0.43	1.12	0.36	0.56
23	0.58	0.58	0.86	0.5	0.64	1.22	0.11	0.65
24	0.15	0.3	0.26	0.11	0.11	0.04	0.36	0.29
25	0.18	0.23	0.91	0.62	0.48	1.12	0.33	0.2
26	0.3	0.29	0.7	0.74	0.37	1.09	1	0.3
27	0.22	0.28	0.18	0.15	0.31	0.18	0.37	0.09
28	0.07	0.34	0.73	0.54	0.6	0.82	0.4	0.29
29	0.21	0.09	0.19	0.91	0.81	0.51	0.63	0.52
30	0.23	0.25	0.37	0.23	0.37	0.3	0.48	0.12
31	0.13	0.28	0.78	0.44	0.85	0.93	0.14	0.11
32	0.3	0.36	0.31	0.5	0.85	0.69	0.38	0.25
33	0.18	0.24	0.36	0.32	0.13	0.23	0.18	0.14
34	0.1	0.07	0.44	0.39	0.5	0.8	0.13	0.2
35	0.37	0.48	0.26	0.55	0.45	0.37	0.62	0.38
36	0.11	0.27	0.24	0.14	0.2	0.37	0.1	0.33
37	0.06	0.01	0.1	0.1	0.21	0.59	0.04	0.38
38	0.31	0.24	0.18	0.29	0.17	0.12	0.12	0.3
39	0.07	0.24	0.18	0.15	0.21	0.18	0.16	0.51
40	0.07	0.05	0.11	0.22	0.21	0.47	0.2	0.32

Table D.3: Input Current Harmonic Components with L_s = 15%

	pf=+30	pf=+20	pf=+10	pf=0	pf=-10	pf=-20	pf=-30	pf=-40
THD	46	38.89	31.65	24.26	16.85	13.05	15.66	20.59
TEHD	44.69	37.27	29.64	21.73	13.91	9.05	12.40	17.61
TOHD	10.89	11.11	11.08	10.80	9.50	9.40	9.57	10.67
0	0.1	0.1	0.07	0.04	0.02	0	0.04	0.06
1	100	100	100	100	100	100	100	100
2	41.36	32.84	24.73	16.75	9.55	2.97	8.15	13.13
3	0.22	0.23	0.11	0.07	0.07	0.07	0.1	0.13
4	15.88	16.72	15.75	13.39	9.02	5.99	7.71	10.96
5	7.89	9.35	10.3	9.98	7.72	6.63	7.37	8.98
6	0.2	0.23	0.14	0.04	0.06	0.02	0.1	0.06
7	6.85	5.52	3.45	3.55	4.72	5.98	5.63	5.37
8	5.14	5.25	3.54	2.75	3.72	5	4.43	3.56
9	0.17	0.22	0.13	0.07	0.05	0.07	0.02	0.13
10	2.19	1.1	2.04	1.66	1.67	2.91	2.47	1.17
11	2.69	1.83	1.62	1.69	1.64	2.25	1.76	1.11
12	0.13	0.2	0.14	0.09	0.12	0.11	0.11	0.14
13	0.79	0.85	0.9	0.59	1.61	1.07	0.42	1.28
14	1.64	1.07	1.15	0.72	1.44	1.1	0.63	1.43
15	0.09	0.16	0.15	0.09	0.1	0.16	0.05	0.16
16	0.28	0.79	0.39	0.6	0.92	0.83	0.44	0.9
17	0.91	0.97	0.77	0.73	1.12	0.74	0.84	0.9
18	0.05	0.11	0.08	0.14	0.07	0.2	0.11	0.14
19	0.42	0.23	0.4	0.33	0.83	0.06	0.82	0.18
20	0.46	0.64	0.63	0.51	0.81	0.38	0.92	0.22
21	0.03	0.08	0.11	0.22	0.1	0.22	0.15	0.07
22	0.38	0.13	0.14	0.26	0.23	0.53	0.23	0.36
23	0.38	0.45	0.35	0.38	0.58	0.41	0.33	0.58
24	0.01	0.05	0.18	0.26	0.21	0.3	0.24	0.04
25	0.32	0.2	0.31	0.26	0.22	1	0.27	0.27
26	0.39	0.36	0.5	0.33	0.34	0.7	0.45	0.41
27	0.02	0.01	0.18	0.32	0.24	0.32	0.29	0.16
28	0.2	0.14	0.28	0.38	0.38	0.6	0.2	0.13
29	0.33	0.19	0.43	0.24	0.73	0.58	0.56	0.21
30	0.03	0.05	0.11	0.38	0.16	0.27	0.25	0.18
31	0.07	0.05	0.2	0.13	0.29	0.42	0.12	0.1
32	0.25	0.14	0.13	0.27	0.45	0.27	0.05	0.22
33	0.03	0.07	0.13	0.26	0.13	0.22	0.31	0.09
34	0.03	0.09	0.15	0.08	0.23	0.33	0.14	0.2
35	0.19	0.25	0.16	0.08	0.15	0.13	0.47	0.25
36	0.03	0.07	0.15	0.04	0.12	0.15	0.3	0.1
37	0.03	0.06	0.02	0.1	0.3	0.1	0.16	0.04
38	0.14	0.25	0.17	0.21	0.32	0.29	0.25	0.22
39	0.02	0.05	0.11	0.06	0.07	0.05	0.19	0.17
40	0.04	0.05	0.08	0.1	0.16	0.09	0.21	0.05

Table D.4: Input Current Harmonic Components with L_s = 20%

	pf=+30	pf=+20	pf=+10	pf=0	pf=-10	pf=-20	pf=-30	pf=-40
THD	48.82	41.56	34.15	26.45	18.53	12.01	12.72	17.18
TEHD	47.87	40.43	32.66	24.47	16.19	8.95	9.76	14.51
TOHD	9.57	9.61	9.97	10.05	9.02	8.02	8.15	9.21
0	0.03	0.04	0.01	0.01	0.01	0.01	0.02	0.03
1	100	100	100	100	100	100	100	100
2	45.49	36.95	28.35	19.94	12.01	4.19	5.51	10.31
3	0.04	0.04	0.05	0.01	0.01	0.02	0.15	0.06
4	14.2	15.64	15.66	13.86	10.46	6.07	6.25	9.28
5	7.06	7.38	9.03	9.54	8.09	5.84	6.12	7.71
6	0.03	0.04	0.006	0.02	0.01	0.03	0.09	0.05
7	5.84	5.59	3.71	2.51	3.63	4.92	5	4.81
8	3.38	4.42	3.83	2.04	2.55	4.35	4.51	3.86
9	0.03	0.03	0.05	0.02	0.01	0.03	0.08	0.03
10	2.4	1.67	1.03	1.87	0.79	1.78	2.11	1.26
11	2.03	2.33	1.31	1.58	1.14	1.69	1.71	0.96
12	0.03	0.02	0.03	0.01	0.02	0.03	0.06	0.05
13	1.46	0.59	1.19	0.71	0.82	1.45	0.45	0.48
14	1.55	1.32	1.19	0.96	0.88	1.61	0.49	0.83
15	0.02	0.02	0.02	0.04	0.01	0.02	0.09	0.04
16	0.61	0.42	0.56	0.53	0.32	0.72	0.37	0.58
17	0.97	0.57	0.84	0.61	0.6	0.87	0.6	0.86
18	0.03	0.02	0	0.02	0.04	0.01	0.09	0.02
19	0.2	0.46	0.03	0.29	0.38	0.19	0.43	0.43
20	0.65	0.41	0.47	0.48	0.48	0.42	0.61	0.57
21	0.02	0.01	0.01	0.02	0.02	0.04	0.1	0.03
22	0.11	0.42	0.25	0.08	0.07	0.27	0.21	0.18
23	0.41	0.41	0.34	0.29	0.34	0.23	0.38	0.23
24	0.01	0	0.02	0.02	0.03	0.03	0.08	0.03
25	0.21	0.24	0.19	0.21	0.19	0.1	0.23	0.1
26	0.25	0.32	0.25	0.28	0.3	0.27	0.4	0.28
27	0.01	0.02	0.02	0.01	0.02	0.03	0.03	0.03
28	0.21	0.08	0.03	0.02	0.03	0.08	0.16	0.14
29	0.19	0.24	0.19	0.17	0.17	0.31	0.21	0.34
30	0.01	0.03	0.03	0.01	0.02	0.03	0.02	0.03
31	0.21	0.06	0.1	0.06	0.11	0.13	0.01	0.12
32	0.17	0.18	0.18	0.16	0.18	0.23	0.13	0.23
33	0.02	0.03	0.02	0.01	0.02	0.02	0.03	0.01
34	0.15	0.08	0.09	0.04	0.03	0.06	0.03	0.03
35	0.16	0.15	0.14	0.14	0.13	0.21	0.22	0.08
36	0.02	0.02	0.01	0.02	0.01	0.02	0.04	0.02
37	0.1	0.05	0.04	0.05	0.06	0.08	0.08	0.05
38	0.15	0.14	0.11	0.12	0.11	0.21	0.18	0.15
39	0.03	0.02	0.01	0.01	0.01	0.01	0.04	0.02
40	0.06	0.03	0.02	0.01	0.02	0.02	0.06	0.04

Table D.5: Input Current Harmonic Components with L_s = 30%

	pf=+30	pf=+20	pf=+10	pf=0	pf=-10	pf=-20	pf=-30	pf=-40
THD	55.37	46.81	38.53	30.57	22.06	12.93	8.39	11.08
TEHD	54.71	46.28	37.76	29.41	20.45	11.13	5.93	8.80
TOHD	8.55	7.08	7.66	8.35	8.27	6.57	5.93	6.75
0	0.05	0.05	0.01	0.04	0.03	0.03	0.02	0
1	100	100	100	100	100	100	100	100
2	53.6	44.42	34.86	25.68	16.58	7.97	1.59	5.43
3	0.1	0.02	0.05	0.03	0.04	0.02	0.13	0.05
4	10.48	12.52	13.95	13.96	11.78	7.49	4.13	5.55
5	7.87	5.22	5.96	7.77	8.07	5.92	4.32	5.27
6	0.05	0.03	0.02	0.03	0.02	0.02	0.1	0.03
7	2.65	4.22	4.19	2.59	0.97	2.5	3.5	3.76
8	2.66	1.97	3.19	3.01	1.16	1.78	3.46	3.75
9	0.01	0.03	0.02	0.02	0.01	0.02	0.09	0.02
10	1.28	2.48	2.02	0.7	1.59	0.57	1.12	1.45
11	1.74	1.57	2.17	1.22	1.37	0.93	1.6	1.7
12	0.02	0.03	0.03	0	0	0.01	0.08	0.02
13	0.62	1.33	0.48	0.81	0.45	0.81	1.05	0.63
14	0.96	0.98	1.11	0.68	0.76	0.73	1.37	0.77
15	0.03	0.02	0.01	0.01	0.01	0.01	0.06	0.01
16	0.31	0.81	0.05	0.56	0.27	0.06	0.44	0.23
17	0.65	0.72	0.56	0.63	0.34	0.37	0.63	0.28
18	0.01	0.01	0.01	0.01	0	0	0.05	0.01
19	0.2	0.4	0.37	0.13	0.31	0.36	0.2	0.16
20	0.43	0.48	0.25	0.36	0.36	0.38	0.4	0.31
21	0.01	0	0.01	0.01	0	0.01	0.04	0.01
22	0.14	0.21	0.36	0.15	0.1	0.06	0.22	0.1
23	0.35	0.35	0.21	0.2	0.17	0.22	0.2	0.4
24	0.01	0	0	0	0.01	0.01	0.03	0.01
25	0.12	0.06	0.3	0.2	0.16	0.18	0.06	0.16
26	0.27	0.24	0.2	0.17	0.15	0.22	0.12	0.34
27	0	0	0.01	0.01	0.01	0.01	0.02	0.01
28	0.09	0.04	0.18	0.08	0.06	0.07	0.09	0.06
29	0.22	0.18	0.18	0.15	0.13	0.14	0.2	0.22
30	0	0	0.01	0.01	0.01	0.01	0.01	0.01
31	0.09	0.06	0.1	0.05	0.08	0.09	0.1	0.04
32	0.16	0.13	0.14	0.11	0.08	0.15	0.16	0.13
33	0	0	0.01	0.01	0	0	0.02	0
34	0.07	0.07	0.09	0.07	0.04	0.06	0.02	0.05
35	0.13	0.1	0.11	0.08	0.08	0.11	0.18	0.07
36	0	0	0.01	0.01	0	0	0.02	0.01
37	0.06	0.06	0.08	0.05	0.05	0.05	0.09	0.04
38	0.09	0.06	0.07	0.08	0.06	0.11	0.13	0.09
39	0.01	0.01	0	0.01	0.01	0.01	0.01	0
40	0.04	0.05	0.07	0.04	0.05	0.06	0.06	0.02

VITA

Alex Joseph Skorcz received his Bachelor of Science in Engineering from Arkansas State University in December of 2005. Upon graduation, he entered the graduate program in the Department of Electrical and Computer Engineering at Texas A&M University where he specialized in Power Electronics and Motor Drives. He received his Master of Science in Electrical Engineering in December of 2007. His research interests include harmonic mitigation, design and control of electrical machines, energy storage systems, and applications of renewable energies.

He can be reached at alex.skorcz@gmail.com or through his advisor Dr. M. Ehsani, Professor, Department of Electrical and Computer Engineering, 3128 TAMU, Texas A&M University, College Station, TX 77843.